

The WASP Model: A Micro-Macro System of Wave-Schrödinger-Plasma Equations for Filamentation

E. Lorin^{1,*}, S. Chelkowski² and A. D. Bandrauk²

¹ School of Mathematics and Statistics, Carleton University, Ottawa, K1S 5B6, Canada.

² Laboratoire de Chimie Théorique, Faculté des Sciences, Université de Sherbrooke, Sherbrooke, J1K 2R1, Canada.

Received 7 October 2009; Accepted (in revised version) 30 April 2010

Communicated by Roger Temam

Available online 27 August 2010

Abstract. In this paper, we model laser-gas interactions and propagation in some extreme regimes. After a mathematical study of a micro-macro Maxwell-Schrödinger model [1] for short, high-frequency and intense laser-gas interactions, we propose to improve this model by adding a plasma equation in order to precisely take into account free electron effects. We examine if such a model can predict and explain complex structures such as *filaments*, on a physical and numerical basis. In particular, we present in this paper a first numerical observation of nonlinear focusing effects using an *ab-initio* gas representation and linking our results with existing nonlinear models.

AMS subject classifications: 35M10, 78A60, 65Z05

Key words: Maxwell equations, Schrödinger equation, laser-gas interaction, filamentation, quantum nonlinear optics.

1 Introduction

We have introduced previously a numerical micro-macro Maxwell-Schrödinger system for the modeling of intense, ultrashort and high frequency laser pulses propagating in dense gaseous media [1, 2]. Numerical simulations were presented in [3–5], where the coupling of the macroscopic Maxwell equations with many Time Dependent Schrödinger Equations (TDSEs), is introduced *via* the exact polarization, thus physically linking the microscopic and macroscopic scales. This numerical model was the first one to our

*Corresponding author. *Email addresses:* elorin@math.carleton.ca (E. Lorin), stephane.chelkowski@USherbrooke.ca (S. Chelkowski), Andre.Bandrauk@USherbrooke.ca (A. D. Bandrauk)

knowledge, that takes into account ionization (short enough pulses) and high order harmonic generation [6,7] at the molecular scale *via* many TDSEs. Usual nonlinear macroscopic models such as Nonlinear Schrödinger Equations (NLS) determine the medium response using macroscopic perturbative expansions. Maxwell-Bloch's equations go beyond the perturbative approach but are restricted to the case of resonantly coupled radiation to a specific transition in the medium.

Consequently, Maxwell-Bloch's equations *a priori* cannot describe various effects we are interested in, such as multiphoton ionization, high order harmonic generation (up to ionization) and then filamentation (that necessitates the inclusion of plasma of free electron effect). The Maxwell-Bloch equations have been mathematically studied by Dumas [8] using some techniques initially introduced for ferromagnetic media [9]. We prove in this paper the existence of weak solutions for the Maxwell-Schrödinger system in a H_2^+ -gas (extension to other gas is straightforward). In contrast to nonlinear Maxwell's equations (see Eqs. (27-29) in [10]) in our approach the nonlinearity appears via medium polarization, which couples the Maxwell and Schrödinger equations which themselves are linear.

The Maxwell equations we consider are linear with constant coefficient but with nonlinear source terms. TDSEs are studied using energy estimates, Grönwall's inequality, classical functional analysis inequalities (Cauchy-Schwarz, Hardy, etc.) and finally Leray-Schauder's fixed point theorem. Note that a fundamental lemma on TDSEs necessary for the proof can be derived from [11]. We also prove that the regularity of the initial data is conserved in time, which is also an important information from a numerical point of view (choice of the numerical method in particular).

After proving the existence of solution, we focus on particular dynamic solutions appearing in nonlinear media called *filaments*. These are defined in [10] as dynamic structures with an intense core, that is able to propagate over extended distances much larger than the typical diffraction length while keeping a narrow beam size without the help of any guiding mechanism. An exhaustive phenomenological and physical description of this phenomenon can be found in [10,12].

In this paper, we wish to establish whether the phenomenon of filamentation is properly predicted by our Maxwell-Schrödinger model. Our model includes ionization properly for very short pulses. In order to describe filamentation for longer laser pulses, commonly used in the experiments, we modify the Maxwell-Schrödinger equations [1] into a so-called Wave-Schrödinger-Plasma (WASP) equations adding an evolution equation on free electrons in order to take precisely plasma effect into account (and the current density in Maxwell's equations). Some elements of proof that filament-like structures can exist for the WASP model are then given. However a scale transform will be ultimately necessary to link our model and results to experimental observations of filamentation over long distances.

We also formally derive from the WASP model some classical nonlinear Schrödinger (NLS) equations that have numerically generated filaments (see [12,13] for instance). Note that some theoretical arguments for proving the existence of filaments for NLS

equations also exist in particular given in [14], however a general theory is still missing. We expect a better understanding of filamentation[†] using the Maxwell-Schrödinger or the WASP equations. Indeed due to TDSEs, the model provides a very precise description of the nonlinear gas response. In this goal, some numerical simulations are provided. In particular, we observe nonlinear focusing effects (key element in filamentation) on an electromagnetic wave (the laser) propagating in *ab initio*-described medium (gas). Filament-like structures are also observed (due to a defocusing).

This paper is organized as follows. In Section 2, we present the Maxwell-Schrödinger model and prove the existence and uniqueness of weak solutions. We improve this model adding an equation for the modeling of plasma of free electron effects. In this section, we also recall and formalize geometrically the notion of filamentation. Some elements of proof that the wave-Schrödinger-plasma model can compute filament-like structures, are given. To illustrate this result, we propose in Section 3, some numerical simulations with the model defined in Section 2. Finally, we offer concluding remarks in Section 4.

2 Wave-Schrödinger-Plasma equations (WASP)

Before introducing the Wave-Schrödinger-Plasma (WASP) equations, we first present the Maxwell-Schrödinger (MS) model initially introduced in [1, 2] and for which existence and uniqueness of weak solutions is proven. The general motivation for developing such models is the non-relevance of usual nonlinear models such as nonlinear wave or Schrödinger equations for the studied regimes [15].

2.1 Maxwell-Schrödinger model and its analysis

2.1.1 Maxwell-Schrödinger model

Mathematically we consider the coupling of the 3d macroscopic Maxwell equations with many Time Dependent Schrödinger Equations (TDSEs). We will work under the dipole approximation, so that the electric field will be supposed to be constant at the molecule scale. This is valid when the smallest internal wavelengths λ_{\min} of the electromagnetic field are much larger than the molecule size ℓ , that is

$$\ell = o(\lambda_{\min}).$$

For the Maxwell equations we will denote by $\Omega \subset \mathbb{R}^3$ the bounded space domain with a smooth boundary Γ and $\mathbf{r} = (x, y, z)^T$ the space variable in Ω . At the molecule scale, we will denote by

$$(\mathbf{r}', R') = (x', y', z', R')^T \in \mathbb{R}^3 \times \mathbb{R}_+,$$

[†]This important phenomenon is source of many potential applications in nanotechnology, laser surgery, air communications, quantum control, dynamical molecular imaging, etc.

the space variable (for electrons and ions). The molecular density is supposed to be constant in time and is given by $\mathcal{N} \in \mathcal{C}_0^\infty(\Omega)$. The equations we consider are the following if the medium is supposed to be neutral,

$$\begin{cases} \partial_t \mathbf{B}(\mathbf{r}, t) = -c \nabla \times \mathbf{E}(\mathbf{r}, t), \\ \partial_t \mathbf{E}(\mathbf{r}, t) = c \nabla \times \mathbf{B}(\mathbf{r}, t) - 4\pi \partial_t \mathbf{P}(\mathbf{r}, t), \\ \nabla \cdot \mathbf{B}(\mathbf{r}, t) = 0, \\ \nabla \cdot (\mathbf{E}(\mathbf{r}, t) + 4\pi \mathbf{P}(\mathbf{r}, t)) = 0, \end{cases} \quad (2.1)$$

with

$$\begin{cases} \mathbf{P}(\mathbf{r}, t) = \mathcal{N}(\mathbf{r}) \sum_{i=1}^m \mathbf{P}_i(\mathbf{r}, t) = \mathcal{N}(\mathbf{r}) \sum_{i=1}^m \chi_{\Omega_i}(\mathbf{r}) \int_{\mathbb{R}^3 \times \mathbb{R}_+} \psi_i(R', \mathbf{r}', t) \mathbf{r}' \psi_i^*(R', \mathbf{r}', t) d\mathbf{r}' dR', \\ i \partial_t \psi_i(R', \mathbf{r}', t) = -\frac{\Delta_{\mathbf{r}'}}{2} \psi_i(R', \mathbf{r}', t) - \frac{\Delta_{R'}}{m_p} \psi_i(R', \mathbf{r}', t) + \theta(R', \mathbf{r}') \cdot \mathbf{E}_{\mathbf{r}'} \psi_i(R', \mathbf{r}', t) \\ + (V_i(R') + V_c(R', \mathbf{r}')) \psi_i(R', \mathbf{r}', t), \quad \forall i \in \{1, \dots, m\}. \end{cases} \quad (2.2)$$

In (2.2), V_c denotes the Coulomb potential, V_i the nucleus potential and θ is a regular vector function with compact support \mathcal{D}_1 equal to \mathbf{r}' on a compact set $\mathcal{D}_2 \subset \mathcal{D}_1$. In the case of a H_2^+ -molecule gas, where the 3-body problem is transformed by symmetry into a 2-body problems, the potentials write

$$V_c(R', \mathbf{r}') = -\frac{1}{\sqrt{x'^2 + (y' - R'/2)^2 + z'^2}} - \frac{1}{\sqrt{x'^2 + (y' + R'/2)^2 + z'^2}} \quad (2.3a)$$

$$V_i(R') = \frac{1}{R'}. \quad (2.3b)$$

Note also that, for other molecules the kinetic operators would also have to be modified. For more complex N -particle molecules, the potential operator of the Schrödinger equation has to be nonlinearly approximated in including the particle interactions: Hartree-Fock, Kohn-Sham, TDDFT models, etc. We finally impose Dirichlet's boundary conditions on Γ :

$$\mathbf{E}(\mathbf{r}, t) = \mathbf{B}(\mathbf{r}, t) = \mathbf{0}, \quad \forall t \geq 0, \quad \forall \mathbf{r} \in \Gamma.$$

In (2.2), Ω_i denotes the macroscopic spatial domain containing a molecule of reference of wavefunction ψ_i , and \mathbf{P}_i denotes the macroscopic polarization associated to this domain. The space Ω_i contains $\mathcal{N}(\mathbf{r}) \text{vol}(\Omega_i)$ molecules represented by ψ_i . Naturally we have

$$\bigcup_{i=1}^m \Omega_i = \Omega.$$

We now assume that the spatial support of ψ_i is included in a domain $\omega_i \subset \mathbb{R}^3 \times \mathbb{R}_+$, that is supposed to be *sufficiently large*, see Fig. 1. In the second part of this paper, we will

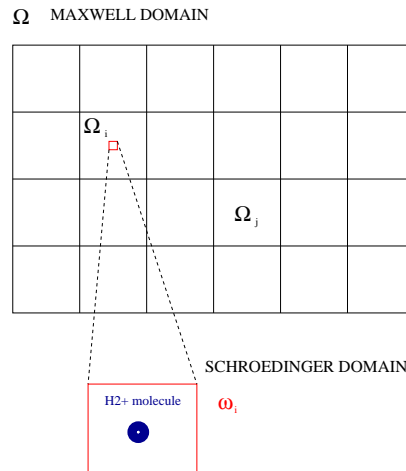


Figure 1: Spatial domains.

allow free electrons to reach the boundary ω_i and we will impose absorbing boundary conditions on $\partial\omega_i$. We refer to [2] for a complete description of the geometry of this model. Functions χ_{Ω_i} are defined by $\chi \otimes \mathbf{1}_{\Omega_i}$ where $\chi \in C_0^\infty(\mathbb{R}^3)$ is a plateau function and $\mathbf{1}_{\Omega_i}$ is the characteristic function of Ω_i . Finally \mathbf{E}_{r_i} denotes the electric field (supposed constant in space) in Ω_i . In the following, we will denote

$$\bar{\psi} = (\psi_1, \dots, \psi_m)^T.$$

2.1.2 Existence and uniqueness of weak solutions for the Maxwell-Schrödinger model

We are interested in this part in proving that the above model is well-posed. We denote by $(\mathbf{E}_0, \mathbf{B}_0, \bar{\psi}_0)^T$ the initial data of the system, where $\bar{\psi}_0 = (\psi_{0,1}, \dots, \psi_{0,m})^T$. We will first suppose that $\mathbf{E}_0, \mathbf{B}_0$ belong to

$$(H^1(\Omega))^3 \quad \text{and} \quad \bar{\psi}_0 \in (H^1(\mathbb{R}^3 \times \mathbb{R}_+) \cap H_1(\mathbb{R}^3 \times \mathbb{R}_+))^m,$$

with the following definition, see [11]:

$$H_1(\mathbb{R}^3 \times \mathbb{R}_+) = \left\{ u \in L^2(\mathbb{R}^3 \times \mathbb{R}_+), \quad \|u\|_{H_1^+} = \int_{\mathbb{R}^3 \times \mathbb{R}_+} (1 + \|(R', \mathbf{r}')^T\|_2^2) |u(R', \mathbf{r}')|^2 dR' d\mathbf{r}' < \infty \right\}.$$

In the following we will respectively denote by L^2, H^1, H_1^+ , the sets $L^2(\mathbb{R}^3 \times \mathbb{R}_+), H^1(\mathbb{R}^3 \times \mathbb{R}_+), H_1(\mathbb{R}^3 \times \mathbb{R}_+)$. We now justify the introduction of such a model by proving its well-posedness for a H_2^+ gas. Note that for other gas which corresponds to change the potentials (2.3), the analysis presented in the proof is *a priori* still valid, but may require additional technical but secondary difficulties.

Theorem 2.1. *Suppose that*

$$(\mathbf{E}_0, \mathbf{B}_0) \in (H^1(\Omega))^3 \times (H^1(\Omega))^3 \quad \text{and} \quad \bar{\psi}_0 \in (H^1(\Omega) \cap H_1^+)^m,$$

with

$$\bar{\psi}(R' = 0, \mathbf{r}', t) = 0 \in \mathbb{R}^m,$$

for all $\mathbf{r}' \in \mathbb{R}^3$ and $t \in \mathbb{R}_+$ and $\mathcal{N} \in C_0^\infty(\Omega)$. Then, there exists a time $T > 0$, for which there exists a unique

$$(\mathbf{E}, \mathbf{B}, \bar{\psi}) \in \left(L^\infty(0, T; (H^1(\Omega))^3) \times H^1(0, T; (L^2(\Omega))^3) \right)^2 \times L^\infty(0, T; (H^1 \cap H_1^+)^m)$$

solution of (2.1), (2.2).

In order to show this results, let us prove some important intermediate results. Note also that in the proof, in order to lighten the notations, we have set $c = 1$ and remove the 4π appearing in (2.1). This change has of course, no consequence on the analysis of existence of weak solutions.

Lemma 2.1. *For all time $T > 0$, we have*

$$\begin{aligned} & \|\mathbf{E}(\cdot, T)\|_{(L^2(\Omega))^3}^2 + \|\mathbf{B}(\cdot, T)\|_{(L^2(\Omega))^3}^2 \\ &= \|\mathbf{E}_0\|_{(L^2(\Omega))^3}^2 + \|\mathbf{B}_0\|_{(L^2(\Omega))^3}^2 - 2 \int_0^T \int_\Omega \mathbf{E}(\mathbf{r}, t) \cdot \partial_t \mathbf{P}(\mathbf{r}, t) d\mathbf{r} dt, \end{aligned} \tag{2.4a}$$

and

$$\begin{aligned} & \|\nabla \cdot \mathbf{E}(\cdot, T)\|_{L^2(\Omega)}^2 + \|\nabla \cdot \mathbf{B}(\cdot, T)\|_{L^2(\Omega)}^2 \\ &= \|\nabla \cdot \mathbf{E}_0\|_{L^2(\Omega)}^2 + \|\nabla \cdot \mathbf{B}_0\|_{L^2(\Omega)}^2 - 2 \int_0^T \int_\Omega \nabla \cdot \mathbf{E}(\mathbf{r}, t) \partial_t \nabla \cdot \mathbf{P}(\mathbf{r}, t) d\mathbf{r} dt. \end{aligned} \tag{2.4b}$$

Proof. As usual, we take the scalar product of

$$\partial_t \mathbf{E}(\mathbf{r}, t) = \nabla \times \mathbf{B}(\mathbf{r}, t) - \partial_t \mathbf{P}(\mathbf{r}, t), \tag{2.5}$$

with \mathbf{E} and we integrate over $[0, T]$ in time and Ω in space, which gives

$$\int_0^T \int_\Omega \mathbf{E}(\mathbf{r}, t) \cdot \partial_t \mathbf{E}(\mathbf{r}, t) = \frac{1}{2} \left(\|\mathbf{E}(\cdot, T)\|_{(L^2(\Omega))^3}^2 - \|\mathbf{E}_0\|_{(L^2(\Omega))^3}^2 \right),$$

and using Dirichlet's boundary conditions, we have

$$\begin{aligned} & \int_0^T \int_\Omega \mathbf{E}(\mathbf{r}, t) \cdot \nabla \times \mathbf{B}(\mathbf{r}, t) \\ &= \int_0^T \int_\Omega \mathbf{B}(\mathbf{r}, t) \cdot \nabla \times \mathbf{E}(\mathbf{r}, t) = - \int_0^T \int_\Omega \mathbf{B}(\mathbf{r}, t) \cdot \partial_t \mathbf{B}(\mathbf{r}, t) \\ &= - \frac{1}{2} \left(\|\mathbf{B}(\cdot, T)\|_{(L^2(\Omega))^3}^2 - \|\mathbf{B}_0\|_{(L^2(\Omega))^3}^2 \right). \end{aligned}$$

This allows to deduce (2.4a). The principle is identical for (2.4b) by taking ∇ of (2.5) and integrating in space and time. \square

Lemma 2.2. *Suppose given*

$$\mathbf{E}(\mathbf{r}, \cdot) \in L^\infty(0, T) \quad \text{and} \quad \partial_t \mathbf{E}(\mathbf{r}, \cdot) \in L^1(0, T),$$

for \mathbf{r} fixed in Ω . Imposing

$$\psi_i(R' = 0, \mathbf{r}', t) = 0,$$

for all $\mathbf{r}' \in \mathbb{R}^3$ and $t \in \mathbb{R}_+$, then, for all $\psi_{0,i} \in H^1 \cap H_1^+$, there exists

$$\psi_i \in L^\infty(0, T; H^1 \cap H_1^+)$$

solution of the last equation of (2.2), and there exists a positive constant C_T such that

$$\|\psi_i\|_{L^\infty(0, T; H^1 \cap H_1^+)} \leq C_T \|\psi_{0,i}\|_{H^1 \cap H_1^+}.$$

Proof. Note that the proof of this lemma follows closely the proof of Theorem 5 from [11]. In the following, we will denote by \mathcal{E} the laser operator, and for fixed \mathbf{r} , $\mathbf{E}(\mathbf{r}, t)$ is denoted by $\mathbf{E}(t)$:

$$\mathcal{E}: (R', \mathbf{r}', t) \mapsto \mathcal{E}(R', \mathbf{r}', t) = \theta(R', \mathbf{r}') \cdot \mathbf{E}(t).$$

In a first time we regularize the potentials, defining with ε a positive constant

$$V_c^\varepsilon(R', \mathbf{r}') = -\frac{1}{\sqrt{\varepsilon^2 + x'^2 + (y' - R'/2)^2 + z'^2}} - \frac{1}{\sqrt{\varepsilon^2 + x'^2 + (y' + R'/2)^2 + z'^2}}$$

$$V_i^\varepsilon(R') = \frac{1}{\sqrt{\varepsilon^2 + R'^2}}.$$

We have

$$|V_c^\varepsilon| \leq |V_c|, \quad |V_i^\varepsilon| \leq |V_i| \quad \text{and} \quad \partial_t V_c^\varepsilon = \partial_t V_i^\varepsilon = 0.$$

Then

$$i\partial_t \psi^\varepsilon(R', \mathbf{r}', t) = \left[-\frac{1}{2} \Delta_{\mathbf{r}'} - \frac{1}{m_p} \Delta_{R'} + V_c^\varepsilon(R', \mathbf{r}') + V_i^\varepsilon(R') + \theta(R', \mathbf{r}') \cdot \mathbf{E}(t) \right] \psi^\varepsilon(R', \mathbf{r}', t). \quad (2.6)$$

As remarked in [11], there exists a unique $\psi^\varepsilon \in C^0(0, T; H^1 \cap H_1^+)$ solution of (2.6), as V_c^ε , V_i^ε , $\theta \cdot \mathbf{E}$ belong to $L^\infty(0, T; C_0^2(\mathbb{R}^3 \times \mathbb{R}_+))$. We now search for an estimate in H_1^+ of ψ^ε . First, we recall that a norm on $H^1 \cap H_1^+$ is (for instance)

$$\|\psi^\varepsilon(t)\|_{H^1 \cap H_1^+}^2 = \int_{\mathbb{R}^3 \times \mathbb{R}_+} \left(|\nabla_{\mathbf{r}'} \psi^\varepsilon|^2 + |\nabla_{R'} \psi^\varepsilon|^2 + (1 + \|(R', \mathbf{r}')\|_2^2) |\psi^\varepsilon|^2 \right).$$

Then there exists a constant $M_p > 0$ ($= 1$ for instance as $m_p > 1$), such that

$$\int_{\mathbb{R}^3 \times \mathbb{R}_+} \left(\frac{|\nabla_{\mathbf{r}'} \psi^\varepsilon|^2}{2} + \frac{|\nabla_{R'} \psi^\varepsilon|^2}{m_p} + (1 + \|(R', \mathbf{r}')\|_2^2) |\psi^\varepsilon|^2 \right) \leq M_p \|\psi^\varepsilon(t)\|_{H^1 \cap H_1^+}. \quad (2.7)$$

The main difficulty consists of finding a positive constant C such that

$$\|\psi^\varepsilon(t)\|_{H^1 \cap H_1^+}^2 \leq C \|\psi_0\|_{H^1 \cap H_1^+}^2. \quad (2.8)$$

Supposing (2.8) is true, using a compactness argument, there exists a sequence ε_n such that

$$\psi^{\varepsilon_n} \xrightarrow[n \rightarrow \infty]{*} \psi, \quad \text{in } L^\infty(0, T; H^1 \cap H_1^+).$$

We finally get

$$\|\psi(t)\|_{H^1 \cap H_1^+}^2 \leq C \|\psi_0\|_{H^1 \cap H_1^+}^2.$$

This would prove the existence of a solution in the distributional sense for Eq. (2.1).

In order to obtain estimate (2.8), it is first necessary to have an estimate of

$$\frac{d}{dt} \int_{\mathbb{R}^3 \times \mathbb{R}_+} \left((1 + \|(R', \mathbf{r}')\|_2^2) |\psi^\varepsilon|^2 \right) \quad \text{and} \quad \frac{d}{dt} \int_{\mathbb{R}^3 \times \mathbb{R}_+} \left(\frac{|\nabla_{\mathbf{r}'} \psi^\varepsilon|^2}{2} + \frac{|\nabla_{R'} \psi^\varepsilon|^2}{m_p} \right).$$

With this aim and as proposed in [11], we multiply the TDSE by $(1 + \|(R', \mathbf{r}')\|_2^2) \psi^{\varepsilon*}$, we integrate on $\mathbb{R}^3 \times \mathbb{R}_+$ using that $\bar{\psi}(R' = 0, \mathbf{r}', t) = 0$, and we finally take the imaginary part

$$\begin{aligned} & \frac{d}{dt} \int_{\mathbb{R}^3 \times \mathbb{R}_+} \left((1 + \|(R', \mathbf{r}')\|_2^2) |\psi^\varepsilon|^2 \right) \\ &= \text{Im} \int_{\mathbb{R}^3 \times \mathbb{R}_+} \left[\nabla_{\mathbf{r}'} \left(\|(R', \mathbf{r}')\|_2^2 \psi^{\varepsilon*} \right) \cdot \frac{\nabla_{\mathbf{r}'} \psi^\varepsilon}{2} + \nabla_{R'} \left(\|(R', \mathbf{r}')\|_2^2 \psi^{\varepsilon*} \right) \cdot \frac{\nabla_{R'} \psi^\varepsilon}{m_p} \right]. \end{aligned}$$

We easily obtain by differentiation and Cauchy-Schwarz inequality that

$$\frac{d}{dt} \int_{\mathbb{R}^3 \times \mathbb{R}_+} (1 + \|(R', \mathbf{r}')\|_2^2) |\psi^\varepsilon|^2 \leq \frac{1}{2} \int_{\mathbb{R}^3 \times \mathbb{R}_+} \left(\|(R', \mathbf{r}')\|_2^2 \psi^{\varepsilon*} + \frac{|\nabla_{\mathbf{r}'} \psi^\varepsilon|^2}{2} + \frac{|\nabla_{R'} \psi^\varepsilon|^2}{m_p} \right).$$

The same manner we multiply by $\partial_t \psi^{\varepsilon*}$ we take the real part and we integrate over $\mathbb{R}^3 \times \mathbb{R}_+$. That is

$$0 = \int_{\mathbb{R}^3 \times \mathbb{R}_+} \text{Re} \left(-\frac{\partial_t \psi^{\varepsilon*} \Delta_{\mathbf{r}'} \psi^\varepsilon}{2} - \frac{\partial_t \psi^{\varepsilon*} \Delta_{R'} \psi^\varepsilon}{m_p} + V_c^\varepsilon \psi^\varepsilon \partial_t \psi^{\varepsilon*} + V_i^\varepsilon \psi^\varepsilon \partial_t \psi^{\varepsilon*} + \mathcal{E} \psi^\varepsilon \partial_t \psi^{\varepsilon*} \right). \quad (2.9)$$

Then

$$\begin{aligned} & \frac{d}{2dt} \int_{\mathbb{R}^3 \times \mathbb{R}_+} \left(\frac{|\nabla_{\mathbf{r}'} \psi^\varepsilon|^2}{2} + \frac{|\nabla_{R'} \psi^\varepsilon|^2}{m_p} \right) \\ &= -\frac{1}{2} \int_{\mathbb{R}^3 \times \mathbb{R}_+} (V_c^\varepsilon + V_i^\varepsilon + \mathcal{E}) \partial_t |\psi^{\varepsilon*}|^2 \\ &= -\frac{d}{2dt} \int_{\mathbb{R}^3 \times \mathbb{R}_+} (V_c^\varepsilon + V_i^\varepsilon + \mathcal{E}) |\psi^{\varepsilon*}|^2 + \frac{1}{2} \int_{\mathbb{R}^3 \times \mathbb{R}_+} \partial_t \mathcal{E} |\psi^\varepsilon|^2. \end{aligned}$$

Trivially there exists a constant C_2

$$\int_{\mathbb{R}^3 \times \mathbb{R}_+} \partial_t \mathcal{E} |\psi^\varepsilon|^2 \leq C_2 \|\partial_t \mathcal{E}\|_{L^\infty(\mathbb{R}^3 \times \mathbb{R}_+)} \|\psi^\varepsilon\|_{H^1 \cap H_1^+}^2.$$

We then obtain the following estimate:

$$\begin{aligned} & \frac{d}{dt} \int_{\mathbb{R}^3 \times \mathbb{R}_+} \left(\frac{|\nabla_{\mathbf{r}'} \psi^\varepsilon|^2}{2} + \frac{|\nabla_{R'} \psi^\varepsilon|^2}{m_p} \right) \\ & \leq \frac{d}{dt} \left[\int_{\mathbb{R}^3 \times \mathbb{R}_+} \left((V_c^\varepsilon + V_i^\varepsilon + \mathcal{E}) |\psi^\varepsilon|^2 \right) \right] + C_2 \|\partial_t \mathcal{E}\|_{L^\infty(\mathbb{R}^3 \times \mathbb{R}_+)} \|\psi^\varepsilon\|_{H^1 \cap H_1^+}^2. \end{aligned} \quad (2.10)$$

Next, setting

$$E_{m_p}^\varepsilon(t) = \int_{\mathbb{R}^3 \times \mathbb{R}_+} \left(\frac{|\nabla_{\mathbf{r}'} \psi^\varepsilon|^2}{2} + \frac{|\nabla_{R'} \psi^\varepsilon|^2}{m_p} + (1 + \|(R', \mathbf{r}')\|_2^2) |\psi^\varepsilon|^2 \right),$$

and because of (2.9) and (2.10), there exists a positive constant C_3 such that

$$\frac{d}{dt} E_{m_p}^\varepsilon(t) \leq \frac{d}{dt} \int_{\mathbb{R}^3 \times \mathbb{R}_+} \left((V_c^\varepsilon + V_i^\varepsilon + \mathcal{E}) |\psi^{\varepsilon*}|^2 \right) + C_3 [1 + \|\partial_t \mathcal{E}\|_{L^\infty(\mathbb{R}^3 \times \mathbb{R}_+)}] E_{m_p}^\varepsilon(t).$$

By integration, we have

$$\begin{aligned} E_{m_p}^\varepsilon(t) & \leq \int_{\mathbb{R}^3 \times \mathbb{R}_+} (V_c^\varepsilon + V_i^\varepsilon + \mathcal{E}(t)) |\psi^\varepsilon(t)|^2 - \int_{\mathbb{R}^3 \times \mathbb{R}_+} (V_c^\varepsilon + V_i^\varepsilon + \mathcal{E}(0)) |\psi^\varepsilon(0)|^2 \\ & \quad + C_3 \int_0^t [1 + \|\partial_t \mathcal{E}\|_{L^\infty(\mathbb{R}^3 \times \mathbb{R}_+)}] E_{m_p}^\varepsilon(s) ds + E_{m_p}^\varepsilon(0). \end{aligned}$$

As by definition of V_i^ε , V_c^ε and V_i , V_c

$$\begin{aligned} \int_{\mathbb{R}^3 \times \mathbb{R}_+} (V_c^\varepsilon + V_i^\varepsilon) |\psi^\varepsilon(t)|^2 & \leq \int_{\mathbb{R}^3 \times \mathbb{R}_+} (|V_c| + |V_i|) |\psi^\varepsilon(t)|^2 \\ & \leq \left(\int_{\mathbb{R}^3 \times \mathbb{R}_+} (|V_c| + |V_i|)^2 |\psi^\varepsilon(t)|^2 \right)^{\frac{1}{2}} \left(\int_{\mathbb{R}^3 \times \mathbb{R}_+} |\psi^\varepsilon(t)|^2 \right)^{\frac{1}{2}}. \end{aligned}$$

By definition of V_i and V_c and by applying Hardy's inequality, there exists two positive constants \tilde{C}_4, C_4 such that (using the definition of V_i and V_c)

$$\begin{aligned} \int_{\mathbb{R}^3 \times \mathbb{R}_+} |\psi^\varepsilon(t)|^2 (|V_c| + |V_i|)^2 &\leq 2 \int_{\mathbb{R}^3 \times \mathbb{R}_+} |\psi^\varepsilon(t)|^2 (V_c^2 + V_i^2) \\ &\leq \tilde{C}_4 \int_{\mathbb{R}^3 \times \mathbb{R}_+} |\nabla_{\mathbf{r}'} \psi^\varepsilon|^2 + |\nabla_{R'} \psi^\varepsilon|^2 \\ &\leq C_4 \|\nabla_{R', \mathbf{r}'} \psi^\varepsilon\|_{L^2(\mathbb{R}^3 \times \mathbb{R}_+)}^2. \end{aligned}$$

So that, by the classical equality $\|\psi_0\|_{L^2}^2 = \|\psi^\varepsilon\|_{L^2}^2$, we have

$$\int_{\mathbb{R}^3 \times \mathbb{R}_+} |\psi^\varepsilon|^2 (V_c^\varepsilon + V_i^\varepsilon)^2 \leq \frac{C_4}{2} \|\nabla_{R', \mathbf{r}'} \psi^\varepsilon\|_{L^2(\mathbb{R}^3 \times \mathbb{R}_+)}^2 + \frac{C_4}{2} \|\psi_0\|_{L^2(\mathbb{R}^3 \times \mathbb{R}_+)}^2. \tag{2.11}$$

Now as $\mathbf{E} \in L^\infty(0, T)$ and $\theta \in C_0^2(\mathbb{R}^3 \times \mathbb{R}_+)$,

$$\int_{\mathbb{R}^3 \times \mathbb{R}_+} |\psi^\varepsilon|^2 \mathcal{E}(t) \leq \|\mathcal{E}\|_{L^\infty(0, T; \mathbb{R}^3 \times \mathbb{R}_+)} \|\psi^\varepsilon(t)\|_{H^1}^2, \tag{2.12}$$

and because of (2.7)

$$E_{m_p}^\varepsilon(0) \leq M_p \|\psi_0\|_{H^1 \cap H_1^+}^2, \tag{2.13}$$

and by definition of V_c and V_i , there exists a positive constant C_5 such that

$$\int_{\mathbb{R}^3 \times \mathbb{R}_+} (V_c^\varepsilon + V_i^\varepsilon + \mathcal{E}(0)) |\psi_0|^2 \leq C_5 \|\psi_0\|_{H^1 \cap H_1^+}^2. \tag{2.14}$$

So that (2.11), (2.12) and (2.13) lead to the existence of 2 positive constants C_6, C_7 such that

$$\|\psi^\varepsilon(t)\|_{H^1 \cap H_1^+}^2 \leq C_6 \|\psi_0\|_{H^1 \cap H_1^+}^2 + C_7 \int_0^t (1 + \|\partial_t \mathcal{E}\|_{L^\infty(0, T; \mathbb{R}^3 \times \mathbb{R}_+)}) \|\psi^\varepsilon(s)\|_{H^1 \cap H_1^+}^2 ds. \tag{2.15}$$

We apply Grönwall's inequality that leads to the existence of a positive constant C_I such that

$$\|\psi^\varepsilon(t)\|_{H^1 \cap H_1^+}^2 \leq C_I \exp \left[\int_0^t (1 + \|\partial_t \mathcal{E}\|_{L^\infty(0, T; \mathbb{R}^3 \times \mathbb{R}_+)}) ds \right] \|\psi_0\|_{H^1 \cap H_1^+}^2. \tag{2.16}$$

Now as $\partial_t \mathbf{E}(\mathbf{r}, \cdot) \in L^1(0, T)$, there exists a constant C such that (2.8) occurs. □

Lemma 2.3. *Suppose given*

$$\mathbf{E}(\mathbf{r}, \cdot) \in L^\infty(0, T) \quad \text{and} \quad \partial_t \mathbf{E}(\mathbf{r}, \cdot) \in L^1(0, T),$$

for \mathbf{r} fixed in Ω . Then, there exists C_T such that for all $\bar{\psi}_0 \in (H^1 \cap H_1^+)^m$, there exists a solution $\bar{\psi} \in L^\infty(0, T; (H^1 \cap H_1^+)^m)$ and

$$\|\bar{\psi}\|_{L^\infty(0, T; (H^1 \cap H_1^+)^m)} \leq C_T \|\bar{\psi}_0\|_{(H^1 \cap H_1^+)^m}.$$

Proof. The previous lemma is valid for all $i = 1, \dots, m$ and by definition $\bar{\psi}$ is equal to $(\psi_1, \dots, \psi_m)^T$. □

Lemma 2.4. For all $T > 0$ and $\bar{\psi} \in (L^\infty(0, T; (H^1 \cap H_1^+)))$,

$$\mathbf{P} \in L^\infty(0, T; (C_0^\infty)^3).$$

Proof. As $\chi_{\Omega_i}, \mathcal{N}$ belong to $C_0^\infty(\Omega)$ and $\psi_i \in L^\infty(0, T; H^1 \cap H_1^+)$, for all $i = 1, \dots, m$, we deduce that

$$t \mapsto \int_{\mathbb{R}^3 \times \mathbb{R}_+} \psi_i(R', \mathbf{r}', t) \mathbf{r}' \psi_i^*(R', \mathbf{r}', t) dR' d\mathbf{r}' \in L^\infty(0, T).$$

In particular for all $i = 1, \dots, m$, as ψ_i belongs to H_1^+ the integral is defined. Finally, by definition of

$$\mathbf{P} = \sum_{i=1}^m \mathbf{P}_i = \sum_{i=1}^m \mathcal{N}(\mathbf{r}) \chi_{\Omega_i}(\mathbf{r}) \int_{\mathbb{R}^3 \times \mathbb{R}_+} \psi_i(R', \mathbf{r}', t) \mathbf{r}' \psi_i^*(R', \mathbf{r}', t) d\mathbf{r}' dR',$$

we deduce the lemma. □

Actually, we have more

Lemma 2.5. For \mathbf{r} fixed in Ω and $T > 0$,

$$\partial_t \mathbf{P}(\mathbf{r}, \cdot) \in L^\infty(0, T) \quad \text{and} \quad \partial_t (\nabla \cdot \mathbf{P}(\mathbf{r}, \cdot)) \in L^\infty(0, T).$$

Proof. First

$$\partial_t \mathbf{P}(\mathbf{r}, t) = \mathcal{N}(\mathbf{r}) \sum_{i=1}^m \partial_t \mathbf{P}_i(\mathbf{r}, t),$$

that is

$$\begin{aligned} \partial_t \mathbf{P}(\mathbf{r}, t) &= \mathcal{N}(\mathbf{r}) \sum_{i=1}^m \partial_t \mathbf{P}_i(\mathbf{r}, t) \\ &= \mathcal{N}(\mathbf{r}) \sum_{i=1}^m \chi_{\Omega_i}(\mathbf{r}) \int_{\mathbb{R}^3 \times \mathbb{R}_+} \partial_t \psi_i(R', \mathbf{r}', t) \mathbf{r}' \psi_i^*(R', \mathbf{r}', t) d\mathbf{r}' dR' \\ &\quad + \mathcal{N}(\mathbf{r}) \sum_{i=1}^m \chi_{\Omega_i}(\mathbf{r}) \int_{\mathbb{R}^3 \times \mathbb{R}_+} \psi_i(R', \mathbf{r}', t) \mathbf{r}' \partial_t \psi_i^*(R', \mathbf{r}', t) d\mathbf{r}' dR'. \end{aligned}$$

As $\psi_i \in L^\infty(0, T; H^1 \cap H_1^+)$, then (using integration by parts) $\partial_t \mathbf{P}_i \in L^\infty(0, T)$ for all i in $\{1, \dots, m\}$ and $\partial_t \mathbf{P} \in L^\infty(0, T)$. Now as $\nabla \cdot \mathbf{P}(\cdot, t) \in C_0^\infty(\Omega)$ at t fixed, we also have that $\partial_t (\nabla \cdot \mathbf{P}(\mathbf{r}', \cdot)) \in L^\infty(0, T)$. □

Lemma 2.6. *There exists a constant $C > 0$ such that for all time $T > 0$,*

$$\sup_{0 \leq t \leq T} \|\mathbf{E}(t)\|_{(H^1(\Omega))^3}^2 + \sup_{0 \leq t \leq T} \|\mathbf{B}(t)\|_{(H^1(\Omega))^3}^2 \leq C. \tag{2.17}$$

Proof. From Lemma 2.1, we have that for all $t \in [0, T]$,

$$\begin{aligned} & \|\mathbf{E}(\cdot, T)\|_{(L^2(\Omega))^3}^2 + \|\mathbf{B}(\cdot, T)\|_{(L^2(\Omega))^3}^2 \\ & \leq \|\mathbf{E}_0(\cdot)\|_{(L^2(\Omega))^3}^2 + \|\mathbf{B}_0(\cdot)\|_{(L^2(\Omega))^3}^2 + 2 \int_0^T \int_{\Omega} |\mathbf{E}(\mathbf{r}, t) \cdot \partial_t \mathbf{P}(\mathbf{r}, t)| \, d\mathbf{r} dt \\ & \leq \|\mathbf{E}_0(\cdot)\|_{(L^2(\Omega))^3}^2 + \|\mathbf{B}_0(\cdot)\|_{(L^2(\Omega))^3}^2 + 2 \int_0^T \int_{\Omega} |\mathbf{E}(\mathbf{r}, t)|^2 \, d\mathbf{r} dt + \int_0^T \int_{\Omega} |\partial_t \mathbf{P}(\mathbf{r}, t)|^2 \, d\mathbf{r} dt, \end{aligned}$$

and

$$\begin{aligned} & \|\nabla \cdot \mathbf{E}(\cdot, T)\|_{L^2(\Omega)}^2 + \|\nabla \cdot \mathbf{B}(\cdot, T)\|_{L^2(\Omega)}^2 \\ & \leq \|\nabla \cdot \mathbf{E}_0\|_{L^2(\Omega)}^2 + \|\nabla \cdot \mathbf{B}_0\|_{L^2(\Omega)}^2 + 2 \int_0^T \int_{\Omega} |\mathbf{E}(\mathbf{r}, t) \cdot \partial_t \nabla \cdot \mathbf{P}(\mathbf{r}, t)| \, d\mathbf{r} dt \\ & \leq \|\nabla \cdot \mathbf{E}_0\|_{L^2(\Omega)}^2 + \|\nabla \cdot \mathbf{B}_0\|_{L^2(\Omega)}^2 + \int_0^T \int_{\Omega} |\mathbf{E}(\mathbf{r}, t)|^2 \, d\mathbf{r} dt + \int_0^T \int_{\Omega} |\partial_t \nabla \cdot \mathbf{P}(\mathbf{r}, t)|^2 \, d\mathbf{r} dt. \end{aligned}$$

In the previous equations, $\|\cdot\|$ denote the L^2 -norm in \mathbb{R}^3 . Using now that

$$\mathbf{P} \in L^\infty(0, T; C_0^\infty(\Omega)^3),$$

we deduce (2.17) using Grönwall's lemma. □

Proof of Theorem 2.1 So far, we have proven that for all $T > 0$, there exists a constant C such that

$$\begin{aligned} & \|\mathbf{E}\|_{L^\infty(0, T; (H^1(\Omega))^3) \cap H^1(0, T; (L^2(\Omega))^3)}^2 + \|\mathbf{B}\|_{L^\infty(0, T; (H^1(\Omega))^3) \cap H^1(0, T; (L^2(\Omega))^3)}^2 \\ & + \|\bar{\psi}\|_{L^\infty(0, T; (H^1 \cap H_1^+)^m)} \leq C. \end{aligned}$$

The boundness of the last term in the above inequality is a consequence of Lemma 2.2. Now as

$$L^\infty(0, T; (H^1(\Omega))^3) \times L^\infty(0, T; (H^1 \cap H_1^+)^m)$$

is compactly embedded in

$$L^2(\Omega \times (0, T]) \times (L^2(\mathbb{R}^3 \times \mathbb{R}_+))^m$$

by Leray-Schauder's fixed point theorem we deduce the existence of a solution for (2.1). The approach is the same as described in [16], we do not detail it. It is based on the

introduction of a continuous mapping easily derived from (2.1), and that depends on a parameter $\lambda \in [0,1]$ and that admits a fixed point in

$$L^2(\Omega \times (0,T]) \times (L^2(\mathbb{R}^3 \times \mathbb{R}_+))^m$$

as verifying Leray-Schauder's theorem assumptions.

Uniqueness is proven by a classical process *via* Grönwall's inequality. Let us set $(\mathbf{E}_1, \mathbf{B}_1, \bar{\psi}_1)^T$ and $(\mathbf{E}_2, \mathbf{B}_2, \bar{\psi}_2)^T$ two solutions of the Cauchy problem (2.1), and

$$(\mathbf{E}, \mathbf{B}, \bar{\psi})^T := (\mathbf{E}_2 - \mathbf{E}_1, \mathbf{B}_2 - \mathbf{B}_1, \bar{\psi}_2 - \bar{\psi}_1)^T$$

with obviously

$$\begin{aligned} (\mathbf{E}(\cdot,0), \mathbf{B}(\cdot,0), \bar{\psi}(\cdot,0))^T &= (\mathbf{0}, \mathbf{0}, \mathbf{0}), \\ \mathbf{P} &:= \mathbf{P}_2 - \mathbf{P}_1, \quad \text{with } \mathbf{P}(\cdot,0) = \mathbf{0}. \end{aligned}$$

We also denote by

$$\bar{\phi} = (\phi_1, \dots, \phi_m)^T := (\psi_{2,1} - \psi_{1,1}, \dots, \psi_{2,m} - \psi_{1,m})^T$$

with then $\bar{\phi}(\cdot,0) = \mathbf{0}$. We naturally have

$$\begin{aligned} \mathbf{P}(\mathbf{r},t) &= \mathcal{N}(\mathbf{r}) \sum_{i=1}^m \mathbf{P}_i(\mathbf{r},t) \\ &= \mathcal{N}(\mathbf{r}) \sum_{i=1}^m \chi_{\Omega_i}(\mathbf{r}) \int_{\mathbb{R}^3 \times \mathbb{R}_+} \mathbf{r}' (|\psi_{i,2}(R', \mathbf{r}', t)|^2 - |\psi_{i,1}(R', \mathbf{r}', t)|^2) d\mathbf{r}' dR'. \end{aligned}$$

Again from

$$\mathbf{E}(\mathbf{r},t) \cdot \partial_t \mathbf{E}(\mathbf{r},t) = \mathbf{E}(\mathbf{r},t) \cdot \nabla \times \mathbf{B}(\mathbf{r},t) - \mathbf{E}(\mathbf{r},t) \cdot \partial_t \mathbf{P}(\mathbf{r},t),$$

we deduce that because $\partial_t \mathbf{P} \in L^\infty(0,T; (C_0^\infty(\Omega))^3)$, there exists $C > 0$ such that

$$\frac{d}{dt} \int_{\Omega} \|\mathbf{E}(\mathbf{r},t)\|_{(L^2(\Omega))^3} d\mathbf{r} + \frac{d}{dt} \int_{\Omega} \|\mathbf{B}(\mathbf{r},t)\|_{(L^2(\Omega))^3} \leq C \int_{\Omega} \|\mathbf{E}(\mathbf{r},t)\|_{(L^2(\Omega))^3}^2 d\mathbf{r},$$

and as for all $i = 1, \dots, m$,

$$\begin{aligned} i \partial_t \phi_i(R', \mathbf{r}', t) &= -\frac{\Delta_{\mathbf{r}'}}{2} \phi_i(R', \mathbf{r}', t) - \frac{\Delta_{R'}}{m_p} \phi_i(R', \mathbf{r}', t) + \theta(R', \mathbf{r}') \cdot \mathbf{E}_{\mathbf{r}'} \phi_i(R', \mathbf{r}', t) \\ &\quad + (V_i(R') + V_c(R', \mathbf{r}')) \phi_i(R', \mathbf{r}', t), \end{aligned}$$

then

$$\begin{aligned} & i \frac{d}{dt} \int_{\mathbb{R}^3 \times \mathbb{R}_+} |\phi_i(R', \mathbf{r}', t)|^2 dR' d\mathbf{r}' \\ &= - \int_{\mathbb{R}^3 \times \mathbb{R}_+} \phi_i^* \Delta_{\mathbf{r}'} \phi_i(R', \mathbf{r}', t) dR' d\mathbf{r}' - 2 \int_{\mathbb{R}^3 \times \mathbb{R}_+} \phi_i^* \frac{\Delta_{R'}}{m_p} \phi_i(R', \mathbf{r}', t) dR' d\mathbf{r}' \\ & \quad + 2 \int_{\mathbb{R}^3 \times \mathbb{R}_+} V_i(R') |\phi_i(R', \mathbf{r}', t)|^2 dR' d\mathbf{r}' + 2 \int_{\mathbb{R}^3 \times \mathbb{R}_+} V_c(R', \mathbf{r}') |\phi_i(R', \mathbf{r}', t)|^2 dR' d\mathbf{r}' \\ & \quad + 2 \int_{\mathbb{R}^3 \times \mathbb{R}_+} \theta(R', \mathbf{r}') \cdot \mathbf{E}_{\mathbf{r}'}(t) |\phi_i(R', \mathbf{r}', t)|^2 dR' d\mathbf{r}'. \end{aligned}$$

By taking the imaginary part and integrating by parts, there exists a positive constant C such that

$$\frac{d}{dt} \int_{\mathbb{R}^3 \times \mathbb{R}_+} |\phi_i(R', \mathbf{r}', t)|^2 dR' d\mathbf{r}' \leq C \int_{\mathbb{R}^3 \times \mathbb{R}_+} |\phi_i(R', \mathbf{r}', t)|^2 \|\nabla_{R', \mathbf{r}'} \phi_i(R', \mathbf{r}', t)\| dR' d\mathbf{r}'.$$

Now as

$$\phi_i \in L^\infty(0, T; H^1 \cap H_1^+) \quad (\text{then } \nabla \phi_i \in L^\infty(0, T; (L^2)^m),$$

we deduce that by Cauchy-Schwarz, there exists $C > 0$ such that

$$\frac{d}{dt} \|\phi_i(t)\|_{L^2(\mathbb{R}^3 \times \mathbb{R}_+)}^2 \leq C \|\phi_i(t)\|_{H^1(\mathbb{R}^3 \times \mathbb{R}_+)}^2,$$

that leads to the existence of $C > 0$ such that

$$\frac{d}{dt} \|\bar{\phi}(t)\|_{(L^2(\mathbb{R}^3 \times \mathbb{R}_+))^m}^2 \leq C \|\bar{\phi}(t)\|_{(H^1(\mathbb{R}^3 \times \mathbb{R}_+))^m}^2.$$

Using the same principle used in the proof Lemma 2.2 (see (2.15)), we can even prove that

$$\frac{d}{dt} \|\bar{\phi}(t)\|_{(H^1(\mathbb{R}^3 \times \mathbb{R}_+))^m}^2 \leq C \|\bar{\phi}(t)\|_{(H^1(\mathbb{R}^3 \times \mathbb{R}_+))^m}^2.$$

In conclusion, there exists $C > 0$ such that

$$\begin{aligned} & \frac{d}{dt} \|\bar{\phi}(t)\|_{(H^1 \cap H_1^+)^m}^2 + \frac{d}{dt} \int_{\Omega} \|\mathbf{E}(\mathbf{r}, t)\|^2 d\mathbf{r} + \|\mathbf{B}(\mathbf{r}, t)\|^2 d\mathbf{r} \\ & \leq C \left(\int_{\Omega} \|\mathbf{E}\|^2 + \|\mathbf{B}\|^2 d\mathbf{r} + \|\bar{\phi}(t)\|_{(H^1 \cap H_1^+)^m}^2 \right). \end{aligned}$$

We conclude by Grönwall using the fact that

$$(\mathbf{E}(\cdot, 0), \mathbf{B}(\cdot, 0), \bar{\phi}(\cdot, 0)) = (\mathbf{0}, \mathbf{0}, \mathbf{0}).$$

The proof is then completed. □

2.2 Laser-gas interaction modeling including plasma of free electrons: the WASP model

In the following two systems of unit will be used: the *International System (s.i.)* and the *Gaussian Centimeter-Gram Second (c.g.s.)* system with *Atomic Units (a.u.)*. The reason is that macroscopic nonlinear Schrödinger or wave models are usually written in *s.i.*, when in the laser-molecule framework, the usual system is *c.g.s.* with *a.u.* We will then work in the *s.i.* system for the classical nonlinear and Schrödinger models introduced in this paper, and in *c.g.s.* for the Maxwell-Schrödinger model that couples macroscopic wave/Maxwell's equations with quantum laser-molecule TDSEs. In each situation, we will clearly identify which system is used in order to avoid any confusion.

2.2.1 Wave-Schrödinger-Plasma equations

Let us now recall that the wave equation for an electric field propagating in a nonhomogeneous medium has the following form (details can be found in the following very complete paper [10]) in *s.i.*:

$$-c^2 \nabla(\nabla \cdot \mathbf{E}) - \partial_{tt}^2 \int_{-\infty}^t n^2(\mathbf{r}, t-t') \mathbf{E}(\mathbf{r}, t') dt' + c^2 \Delta \mathbf{E} = c^2 \mu_0 (\partial_{tt}^2 \mathbf{P}_{nl} + \partial_t \mathbf{J}), \quad (2.18)$$

where n^2 is the linear index of refraction (vacuum and bound electrons), \mathbf{P}_{nl} is the nonlinear polarization associated to bound electrons, \mathbf{J} is the plasma current density associated to free electrons. Using the perturbation theory (see for instance [17]), the term n^2 is usually modeled by $1 + \varepsilon_0 \chi^{(1)}$ and \mathbf{P}_{nl} is modeled by

$$\varepsilon_0 \int \chi^{(3)}(t-t') |\mathbf{E}|^2 \mathbf{E}(t') dt',$$

where the linear and cubic susceptibility tensors $\chi^{(1)}$ and $\chi^{(3)}$ are in a first approximation often supposed to be constant (in space and time which simplify the expression and computation of \mathbf{P}_{nl}). Coefficients ε_0 and μ_0 are respectively the vacuum permittivity and permeability. In that case, vibrations and rotations are neglected (Raman effect), see [18]. $\partial_t \mathbf{J}$ is modeled by $-e^2 \rho E / m_e$, where e is the electron charge, m_e its mass and ρ the electron density (see again [10]). So that (2.18) can be rewritten as:

$$\partial_{tt}^2 \mathbf{E} - c^2 \Delta \mathbf{E} + c^2 \nabla(\nabla \cdot \mathbf{E}) = -c^2 \mu_0 \partial_{tt}^2 \mathbf{P}_E,$$

where

$$\mathbf{P}_E = \varepsilon_0 \chi^{(1)} \mathbf{E} + \varepsilon_0 \chi^{(3)} |\mathbf{E}|^2 \mathbf{E} + \rho \mathbf{E}.$$

That is the modeling for propagation in a nonlinear medium consists of introducing some real tensors (environmental parameter tensors) $(\tilde{\alpha}_i)_i$, such that

$$\partial_{tt}^2 \mathbf{E} - c^2 \Delta \mathbf{E} + c^2 \nabla(\nabla \cdot \mathbf{E}) = \partial_{tt}^2 \tilde{\mathbf{P}}_E, \quad (2.19)$$

where

$$\tilde{\mathbf{P}}_E = \tilde{\alpha}_1 \mathbf{E} + \tilde{\alpha}_2 \rho \mathbf{E} + \tilde{\alpha}_3 |\mathbf{E}|^2 \mathbf{E}. \quad (2.20)$$

Usual models do not go further third order nonlinearities due to: difficulty for modeling high nonlinear coefficients (medium and time dependent), for proving mathematical and physical properties, and for finding accurate and stable numerical approximations for systems with high order nonlinearities, etc. Third order models allow for instance to reproduce the Kerr effect (self-focusing, cubic term). Much more elaborated models can also be found in [10, 12].

Let us now define the Wave-Schrödinger-Plasma equations (WASP) derived from (2.1) and (2.2) in *c.g.s.* as

$$\partial_{tt}^2 \mathbf{E} - c^2 \Delta \mathbf{E} + c^2 \nabla (\nabla \cdot \mathbf{E}) = -4\pi (\partial_{tt}^2 \mathbf{P}_E + \partial_t \mathbf{J}), \quad (2.21)$$

where \mathbf{P}_E is computed as in (2.1), (2.2) and with the same geometrical domains. We assume here that a plasma can be created by free electrons. As is well known the current created by free electrons at the quantum scale is given by

$$\int_{\omega_i} \psi^* \nabla \psi - \psi \nabla \psi^*.$$

In other words, plasma effects (due to ionization) are included in the model *as long as free electrons are not absorbed on* $(\partial\omega_i)_i$ (see Section 2). At the macroscopic scale, the current density and following the above strategy, is given by

$$-e \mathcal{N}(\mathbf{r}') \mathbf{1}_{\Omega_i}(\mathbf{r}') \int_{\omega_i} \psi^* \mathbf{i} \nabla \psi.$$

In the following, we impose absorbing boundary conditions on $\partial\omega_i$ for all $i \in \{1, \dots, m\}$ supposing that the support of ψ_i can reach $\partial\omega_i$ (very intense electric fields, long, or even intense but low frequency pulses). That is, for ε small enough, we define a regular decreasing function f_ε , from 1 for (R', \mathbf{r}') such that

$$d((R', \mathbf{r}'), \partial\omega_i) = \varepsilon,$$

to 0 for all $(R', \mathbf{r}') \in \partial\omega_i$. We multiply ψ_i by f_ε for all (R', \mathbf{r}') such that

$$d((R', \mathbf{r}'), \omega_i) \leq \varepsilon.$$

Such a function can easily be constructed, see [3]. Because of absorbing boundary conditions $\|\psi_i(t)\|_{L^2(\omega_i)}$ is no more constant in time, see Fig. 2.

We model the evolution of free electrons by the following equation:

$$\partial_t \rho(\mathbf{r}, t) + \nabla \cdot (\rho \mathbf{v}_E)(\mathbf{r}, t) = -\mathcal{N}(\mathbf{r}) \sum_{i=1}^m \chi_{\omega_i}(\mathbf{r}) \partial_t \|\psi_i(t)\|_{L^2(\omega_i)}. \quad (2.22)$$

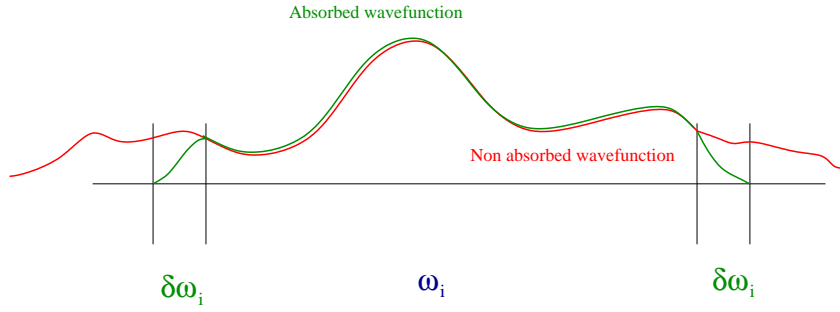


Figure 2: Free electron absorption for domain $\partial\omega_i$ and wavefunction ψ_i : 1d cut.

The source term represents the free electron (unbound) "production". Note that when the molecules are totally ionized in ω_i , the r.h.s is zero, meaning that all the electrons are free ($\psi_i = 0$). Inversely if the electric field intensity is too low to produce ionization, the time derivative of $\|\psi_i(t)\|_{L^2(\omega_i)}$ is zero, corresponding also to a zero free electron production in Ω_i . The time process is more generally the following. In ω_i , when the electric field is intense enough then $-\mathcal{N}(\mathbf{r})\partial_t\|\psi_i(t)\|_{L^2(\omega_i)}$ free electrons are released from Ω_i . Note that this free electron evolution model is very similar to classical ones such as in [10] or [18], where however the free electron production is given by a macroscopic term involving the number of photons in the multi-ionization. The l.h.s. represents the transport of free electrons driven by the electric field \mathbf{E} at a velocity \mathbf{v}_E whose evolution, as a function of \mathbf{E} , ρ and \mathbf{B} is for instance detailed in [12]. In practice, for high frequency fields (respectively for fields initially polarized transversely to the propagation direction z), we assume

$$\nabla(\rho\mathbf{v}_E) \sim \mathbf{0}.$$

The equation modeling the current density evolution is (with $e = m_e = 1$ in *a.u.*), after having neglected the ponderomotive forces

$$\partial_t\mathbf{J} + \frac{1}{\tau_c}\mathbf{J} = \frac{e^2}{m_e}\rho\mathbf{E}, \quad (2.23)$$

where τ_c is the collision time (see again [12]). Note that when pulses are short enough (typically less than $20fs$) in small density plasmas, the collision term can also be neglected in (2.23).

Remark 2.1. At the discrete level, in order to avoid or to limit spurious numerical reflections, discrete absorbing boundary conditions are often used for solving time dependent Schrödinger equations (see [3], for instance).

Due to ionization, the Gauss equation becomes

$$\nabla \cdot (\mathbf{E}(\mathbf{r},t) + 4\pi\mathbf{P}(\mathbf{r},t)) = e(\rho_I(\mathbf{r},t) - \rho(\mathbf{r},t)),$$

where ρ_I is the ion density (if the medium is not neutral) and $e = 1$. The WASP model corresponds to Eqs. (2.21)-(2.23).

Remark 2.2. Following the approach proposed in [1], we present here the semi-discrete approach for solving (2.21)-(2.23) on a spatial domain Ω , which is supposed to be polygonal, to simplify the notations. We assume that \mathbf{E} is constant in space in each mesh cell $\Omega_{h,i}$, ($i=1, \dots, m$) and equal to $\mathbf{E}_{h,i}(\cdot)$, where

$$\Omega_h = \bigcup_{i=1}^m \Omega_{h,i} = \Omega \quad (\text{index } h \text{ refers to discrete version of variables and operators}).$$

We choose $\Omega_{h,i} = \Omega_i$ (with notations of Section 2.1) and we denoted by Δ_h the approximate Laplace operator and by ∇_h the approximate gradient, so that for $t \in [t_n, t_{n+1}]$, we have

$$\begin{aligned} & \partial_{tt}^2 \mathbf{E}_h^{(n)}(t) - c^2 \Delta_h \mathbf{E}_h^{(n)}(t) + c^2 \nabla_h (\nabla_h \cdot \mathbf{E}_h^{(n)}(t)) \\ &= \partial_{tt}^2 \left((\tilde{\alpha}_1 + \tilde{\alpha}_2 \rho_h^{(n)}(t)) \mathbf{E}_h^{(n)}(t) + \tilde{\alpha}_3 |\mathbf{E}_h^{(n)}(t)|^2 \mathbf{E}_h^{(n)}(t) \right), \end{aligned} \quad (2.24)$$

with $\rho_h^{(n)}$ discrete free electron density

$$\begin{aligned} \mathbf{E}_h^{(n)} : t \in [t_n, t_{n+1}] &\mapsto \mathbf{E}_h^{(n)}(t) = \sum_{i=1}^m \mathbf{1}_{\Omega_{h,i}} \mathbf{E}_{h,i}^{(n)}(t), \\ \mathbf{E}_h^{(n+1)} &= \mathbf{E}_h^{(n)}(t_{n+1}). \end{aligned}$$

The semi-discrete approximation of the WASP model can be expressed as

$$\partial_{tt}^2 \mathbf{E}_h^{(n)}(t) - c^2 \Delta_h \mathbf{E}_h^{(n)}(t) + c^2 \nabla_h (\nabla_h \cdot \mathbf{E}_h^{(n)}(t)) = -4\pi (\partial_{tt}^2 \mathbf{P}_h^{(n)}(t) + \partial_t \mathbf{J}_h^{(n)}(t)). \quad (2.25)$$

The polarization is computed from the Schrödinger equations by

$$\mathbf{P}(\mathbf{r}, t) = \mathcal{N}(\mathbf{r}) \sum_{i=1}^m \mathbf{P}_i(\mathbf{r}, t) = \mathcal{N}(\mathbf{r}) \sum_{i=1}^m \chi_{\Omega_i}(\mathbf{r}) \int_{\mathbb{R}^3 \times \mathbb{R}_+} \psi_i(R', \mathbf{r}', t) \mathbf{r}' \psi_i^*(R', \mathbf{r}', t) dR' d\mathbf{r}', \quad (2.26)$$

where $(\psi_i)_i$ are computed by using a Crank-Nicolson scheme.

2.2.2 Maxwell-Schrödinger-Plasma model

The WASP model presented above is obviously partially derived from the Maxwell equations. The general model called the Maxwell-Schrödinger-Plasma is naturally given by:

$$\begin{cases} \partial_t \mathbf{B}(\mathbf{r}, t) = -c \nabla \times \mathbf{E}(\mathbf{r}, t), \\ \partial_t \mathbf{E}(\mathbf{r}, t) = c \nabla \times \mathbf{B}(\mathbf{r}, t) - 4\pi (\partial_t \mathbf{P}(\mathbf{r}, t) + \mathbf{J}(\mathbf{r}, t)), \\ \nabla \cdot \mathbf{B}(\mathbf{r}, t) = 0, \\ \nabla \cdot (\mathbf{E}(\mathbf{r}, t) + 4\pi \mathbf{P}(\mathbf{r}, t)) = e(\rho_I - \rho), \end{cases}$$

with

$$\left\{ \begin{aligned} \mathbf{P}(\mathbf{r},t) &= \mathcal{N}(\mathbf{r}) \sum_{i=1}^m \mathbf{P}_i(\mathbf{r},t) = \mathcal{N}(\mathbf{r}) \sum_{i=1}^m \chi_{\Omega_i}(\mathbf{r}) \int_{\mathbb{R}^3 \times \mathbb{R}_+} \psi_i(R',\mathbf{r}',t) \mathbf{r}' \psi_i^*(R',\mathbf{r}',t) d\mathbf{r}' dR', \\ i \partial_t \psi_i(R',\mathbf{r}',t) &= -\frac{\Delta_{\mathbf{r}'}}{2} \psi_i(R',\mathbf{r}',t) - \frac{\Delta_{R'}}{m_p} \psi_i(R',\mathbf{r}',t) + \theta(R',\mathbf{r}') \cdot \mathbf{E}_{\mathbf{r}_i} \psi_i(R',\mathbf{r}',t) \\ &\quad + (V_i(R') + V_c(R',\mathbf{r}')) \psi_i(R',\mathbf{r}',t), \quad \forall i \in \{1, \dots, m\}, \end{aligned} \right.$$

coupled with

$$\begin{aligned} \partial_t \rho(\mathbf{r},t) &= -\mathcal{N}(\mathbf{r}) \sum_{i=1}^m \chi_{\omega_i}(\mathbf{r}) \partial_t \|\psi_i(t)\|_{L^2(\omega_i)}, \\ \partial_t \mathbf{J} + \frac{1}{\tau_c} \mathbf{J} &= \frac{e^2}{m_e} \rho \mathbf{E}. \end{aligned}$$

The Maxwell-Schrödinger-Plasma model will be used for our numerical simulations in order to have as much physical information as possible. However the WASP model also constitutes a precise and alternative to the Maxwell-Schrödinger-Plasma model.

2.2.3 From WASP to nonlinear wave equation: a conjecture

We want to establish in this section that from the Wave-Schrödinger-Plasma (WASP) equations (2.21) and (2.22), we could derive some nonlinear wave equations taking into account high order nonlinearities, harmonics and ionization. Recall that the main advantage of the WASP model is that environmental parameters are computed using the quantum Schrödinger equations, which allows to obtain realistic parameters (susceptibility tensors) particularly hard to determine for ionized gaseous media for instance. From phenomenological and numerical observations and studies (see [6, 19, 20] for instance) and also formally proven by perturbation theory in [17], we can state the following fundamental result:

Theorem 2.2. *Suppose that ψ is a solution of the TDSE (in c.g.s.)*

$$i \partial_t \psi(\mathbf{r}',t) = -\frac{\Delta_{\mathbf{r}'}}{2} \psi(\mathbf{r}',t) + (V_c(\mathbf{r}') + \mathbf{r}' \cdot \mathbf{E}(t)) \psi(\mathbf{r}',t), \tag{2.27}$$

where $\mathbf{E}(t)$ is given by $\sum_p \mathbf{E}(\omega_p) e^{-i\omega_p t}$. Then there exists a sequence of tensors $\chi^{(i)}$ of order $i+1$, such that the molecule dipole moment is given by

$$\begin{aligned} \mathbf{p}(t) &= \int_{\mathbb{R}^3 \times \mathbb{R}_+} \psi(R',\mathbf{r}',t) \mathbf{r}' \psi^*(R',\mathbf{r}',t) dR' d\mathbf{r}' \\ &= \sum_i \int \chi^{(i)}(t'_1, \dots, t'_i) \cdot \mathbf{E}(t-t'_1) \cdots \mathbf{E}(t-t'_i) dt'_1 \cdots dt'_i, \end{aligned} \tag{2.28}$$

or denoting $x_1 = x'$, $x_2 = y'$ and $x_3 = z'$, the Fourier transform in time of the dipole moment is

$$\begin{aligned} \widehat{d}_k(\omega) &= \mathbb{F} \left(\int_{\mathbb{R}^3 \times \mathbb{R}_+} \psi(R', \mathbf{r}', t) x_k \psi^*(R', \mathbf{r}', t) dR' d\mathbf{r}' \right) \\ &= \sum_{\alpha_1 \cdots \alpha_j} \int \cdots \int \chi_{x_k \alpha_1 \cdots \alpha_j}^{(i)} \left(-\sum_{l=1}^j \omega_l; \omega_1, \dots, \omega_j \right) \widehat{E}_{\alpha_1}(\omega_1) \cdots \widehat{E}_{\alpha_j}(\omega_j) \delta \left(\omega - \sum_{l=1}^j \omega_l \right) d\omega_1 \cdots d\omega_j. \end{aligned} \quad (2.29)$$

This result is based on the perturbation theory apply to the solution of (2.27). This result gives (weak electric fields) a decomposition in nonlinearities and harmonics of the dipole moments, that is on the polarization. The usual assumption consists of neglecting harmonics and nonlinearities beyond the third one (Kerr effect). For instance as shown in [18], the classical perturbation theory leads to (for an incoming pulse of frequency ω_0)

$$\begin{aligned} \mathbf{P}^{(3)}(\mathbf{r}, t) &= C(\omega_0, k_0) \left(3\chi^{(3)}(-\omega_0; \omega_0, -\omega_0, \omega_0) |\mathcal{E}|^2 \mathcal{E} e^{i(k_0 z - \omega_0 t)} \right. \\ &\quad \left. + \chi^{(3)}(-3\omega_0; \omega_0, \omega_0, \omega_0) (\mathcal{E} \cdot \mathcal{E}) \mathcal{E} e^{i(3k_0 z - 3\omega_0 t)} \right), \end{aligned}$$

where \mathcal{E} is the envelope of the electric field and C a constant that depends on $\omega_0, \mu_0, \varepsilon_0, k_0$. Note that

$$\chi^{(3)}(-3\omega_0; \omega_0, \omega_0, \omega_0) \quad \text{and} \quad \chi^{(3)}(-\omega_0; \omega_0, -\omega_0, \omega_0),$$

correspond to the relevant components of $\chi^{(3)}$. In practice, it is often assumed that the third order harmonic (last term of the r.h.s.) is negligible because too weak, with a large phase mismatching. Such an approximate $\mathbf{P}^{(3)}$ then leads to the usual cubic nonlinear Schrödinger equation.

Remark 2.3. As is well-known in centrosymmetric media, even harmonics cancel.

We now state a fundamental conjecture.

Conjecture 1. Theorem (2.2) is still valid for intense and high frequency incoming electric fields. Moreover, the electric field spectrum possesses a plateau (HOHG) then a cut-off frequency, beyond which the harmonics are negligible.

Of course the perturbation theory is *a priori* not valid anymore for intense pulses and the susceptibility tensors from (2.2), which values can be found in [17], are different. One of the key point is the fact that high order harmonics/nonlinearities should not *a priori* be neglected as it is usually done in nonlinear models. Again and as reminded in [17] and performed by Corkum [7], a free electron motion approach is more appropriate.

Some elements of proofs of Conjecture 1

1. For very intense and high frequency incoming electric fields, we can illustrate the fact that high order harmonics and nonlinearities should not necessarily be neglected, by using numerical simulations of laser-molecule interactions by time dependent

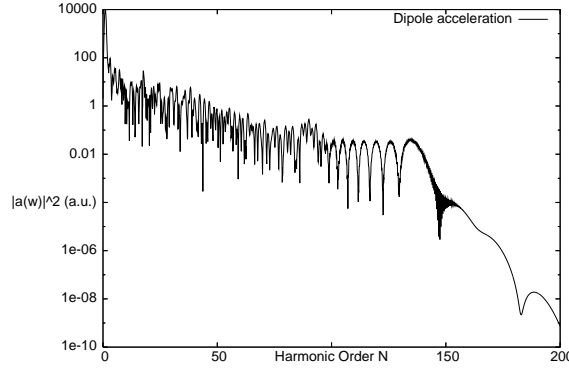


Figure 3: High order harmonic generation in the dipole acceleration.

Schrödinger equations (Fig. 3 in the same framework as Conjecture 1). We represent the dipole acceleration frequencies (\mathbb{F} , Fourier transform in time)

$$\widehat{a}(\omega) = \mathbb{F} \left(\int |\psi(r', t)|^2 \left(-\frac{\partial V_c}{\partial r'} + E(t) \right) dr' \right), \quad (2.30)$$

after a 5-cycle laser pulse interaction with a H_2^+ -molecule. Details can be found in [5], for instance. We clearly identify beyond the incoming laser frequency, a frequency plateau, then a cut-off.

2. We here precise the above remark. With the same assumptions as above, it has been conjectured by Corkum in [7] that there exists an integer N_c , such that the cut-off frequency in (2.30) is located around

$$N_c \omega_0 \sim 3.17 U_p + I_p, \quad (2.31)$$

where ω_0 is the frequency of the incoming pulse, I_p is the ionization potential of the atom/molecule,

$$U_p = \frac{e^2 |E_0|^2}{4m\omega_0^2}$$

is the ponderomotive energy of an electron in an oscillatory field

$$E(t) = E_0 \cos(\omega_0 t)$$

of maximum intensity $eE_0^2/8\pi$. This result has been confirmed experimentally, and numerically on quantum Schrödinger equations (see above). We shortly recall here the principle. Using a classical mechanics 1d model of the electron in a scalar electric field $E(t) = E_0 \cos(\omega_0 t)$, we have from Newton's law

$$\begin{cases} \ddot{y}(t) = -E(t), \\ y(t_0) = 0, \quad \dot{y}(t_0) = 0. \end{cases}$$

The solution at time t_f is naturally given by

$$y(t_f) = \left(\frac{E_0}{\omega_0} \sin(\phi_0) \right) \frac{\phi_f - \phi_0}{\omega_0} + (\cos(\phi_f) - \cos(\phi_0)) \frac{E_0}{\omega_0^2},$$

where $\phi_0 = \omega_0 t_0$, $\phi_f = \omega_0 t_f$ and with

$$\ddot{y}(t_f) = \frac{E_0}{\omega_0} (\sin(\phi_0) - \sin(\phi_f)).$$

We denote by t_f the time such that

$$y(t_f) = y(t_0),$$

that corresponds to the coming back of the particle to its initial position (leading to recombination). We now search for the maximal kinetic energy

$$E_f = \frac{\dot{y}(t_f)^2}{2} = \frac{E_0^2}{2\omega_0^2} (\sin(\phi_0) - \sin(\phi_f))^2 = 4U_p (\sin(\phi_0) - \sin(\phi_f))^2.$$

It can be proven that the maximum admissible maximum is reached for $(\sin(\phi_0) - \sin(\phi_f))^2 \sim 3.17$ (see [6]), to which we add I_p , the ionization potential (tunnel effect). This leads to the maximal frequency for the electric field

$$N_c \omega_0 \sim 3.17 U_p + I_p.$$

This is of course an approximate model as it is based on classical mechanics and for which the electric field propagates in vacuum, but it gives an outstandingly precise description. In practice, as shown numerically in [5], this limit can be exceeded if the gas is dense enough, due to spectral broadening (Kerr). Another way to extend this limit is to couple intense laser pulses (multicolor pulses). However this simple model is not sufficient to describe more complex situations, see [21]. In 1d, this result leads us to conjecture the existence of a sequence of real functions $(\beta_i)_i$ such that

$$\int_{\mathbb{R}} \psi(r', t) r' \psi^*(r', t) dr' \sim \sum_{k=1}^{N_c} E_0^i \beta_i(t) \cos(\omega_0 i t),$$

with

$$\|\beta_{N_c+1}\|_{\infty} = o(\|\beta_i\|_{\infty})$$

for all i in $[1, N_c]$. The cut-off frequency function only involves high order frequencies (around $N_c \omega_0$). Indeed some frequencies (not necessarily all) are excited, between ω_0 and $N_c \omega_0$. By definition of \mathbf{E} and 3d extension, this leads us to conjecture the existence of a sequence of real tensors χ_i of order $i+1$ such that (2.28).

3. Some numerical simulations will be presented in the next section, illustrating Conjecture 1.

Conjecture 1 leads to the following corollary:

Corollary 2.1. From system (2.21)-(2.22), we can derive a nonlinear wave equation, with high order nonlinearities and saturation terms.

Proof. As

$$\mathbf{P}(\mathbf{r}, t) = \mathcal{N}(\mathbf{r}) \sum_{i=1}^m \chi_{\Omega_i}(\mathbf{r}) \int_{\mathbb{R}^3 \times \mathbb{R}_+} \psi_i(R', \mathbf{r}', t) \mathbf{r}' \psi_i^*(R', \mathbf{r}', t) d\mathbf{r}' dR' \quad (2.32)$$

using Theorem 2.2, we can rewrite (2.32)

$$\mathbf{P}(\mathbf{r}, t) = \mathcal{N}(\mathbf{r}) \left(\sum_{k=1}^m (\mathbf{1}_{\Omega_k}(\mathbf{r}) \sum_i \int \chi_k^{(i)}(t'_1, \dots, t'_i) \cdot \mathbf{E}_k(t-t'_1) \cdots \mathbf{E}_k(t-t'_i) dt'_1 \cdots dt'_i) \right) \quad (2.33)$$

with

$$\partial_{tt}^2 \mathbf{E}(\mathbf{r}, t) - c^2 \Delta \mathbf{E}(\mathbf{r}, t) + c^2 \nabla (\nabla \cdot \mathbf{E}(\mathbf{r}, t)) = -4\pi (\partial_{tt}^2 \mathbf{P}(\mathbf{r}, t) + \partial_t \mathbf{J}(\mathbf{r}, t)).$$

This is a formal generalization of the nonlinear wave equation model, from which we can derive nonlinear Schrödinger equations. \square

2.3 About filamentation

We give here a phenomenological definition of filaments and filamentation. Our motivation is to try to characterize these structures, and study if our model will be able to predict them. Note that a scale transform ($x^* = Lx, t^* = Tt, \dots$) in our model is ultimately necessary for comparing our simulations with the experiments. This general formalism that will be useful to guide our numerical simulations and explain the obtained results.

Definition 2.1. [Couairon & Mysyrovicz, 2007] The term filament or filamentation denotes a dynamic structure with an intense core, that is able to propagate over extended distances much larger than the typical diffraction length while keeping a narrow beam size without the help of any external guiding mechanism.

Note that as precised in [10], a constraint on the intensity can be added: the term *filament* describes the part of propagation during which the pulse generates a column of weakly ionized plasma in its wake. Remark that in [22] are also defined Optical Vortex Solitons (OVS) and Localized Optical Vortex Solitons (LOVS) as filaments, although they are defined as zero intensity center solution surrounded by a bright infinite background and nonzero asymptotes at infinity (LOVS). As is commonly admitted, the two main ingredients of filamentation are the optical Kerr effect (self-focusing effect) and multiphoton absorption that limits (saturation) locally the power of the beam (defocusing). Although these two effects have a crucial role we are overall interested in knowing if and how, other important effects can be involved in filament creation and propagation. Giving a mathematical definition of filamentation is very hard, as we have to translate in a rigorous way these features. An attempt of definition for single filaments is as follows. Note that this definition is not exhaustive but allows to identify certain structures as filaments.

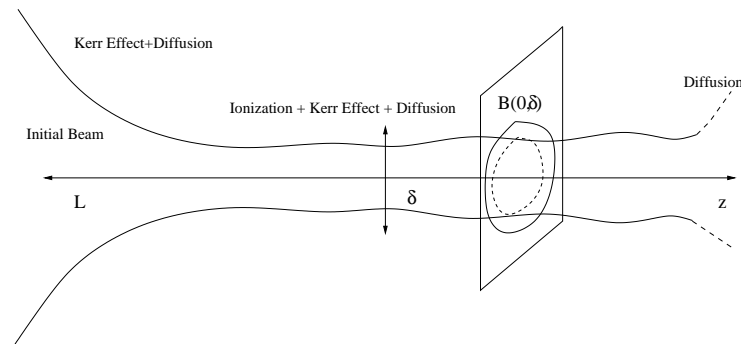


Figure 4: Single filament evolution.

Definition 2.2. (Geometric definition) A solution \mathbf{E} of a nonlinear optics model for laser-gas interaction and propagating along \mathbf{e}_z is a z -filament (Fig. 4) of diameter δ and length L if for all ε small enough, it satisfies the following conditions. Denoting by $B(0,\delta)$ the ball of \mathbb{R}^2 of center $(0,0)$ and diameter δ , and by $\tau_{\tilde{z}} > 0$ with $\tilde{z} \in [0,L]$ fixed, the times (not necessarily unique) such that

$$\max_{t \in \mathbb{R}_+} \int_{B(0,\delta)} \|\mathbf{E}(x,y,\tilde{z},t)\|^2 dx dy = \int_{B(0,\delta)} \|\mathbf{E}(x,y,\tilde{z},\tau_{\tilde{z}})\|^2 dx dy$$

with $\|\cdot\|$ denoting the L^2 -norm on \mathbb{R}^3 :

1. For all $\tilde{z} \in [0,L]$ and $t \in \mathcal{V}(\tau_{\tilde{z}})$ a neighborhood of $\tau_{\tilde{z}}$, we have

$$\frac{\int_{\mathbb{R}^2 - B(0,\delta)} \|\mathbf{E}(x,y,\tilde{z},t)\|^2 dx dy}{\int_{\mathbb{R}^2} \|\mathbf{E}(x,y,\tilde{z},t)\|^2 dx dy} < \varepsilon.$$

2. $L = \mathcal{O}(\delta^{-1})$.

3. For all $\tilde{z} \in [0,L]$ and $t \in \mathcal{V}(\tau_{\tilde{z}})$ and there exists η less than δ such that for all (x,y) in $B(0,\eta)$,

$$\mathbf{E}(x,y,\tilde{z},t) \neq \mathbf{0}.$$

In practice the filament will be admissible if L is "large" enough and δ "small" enough. Note that 1 corresponds to the condition on the beam size that has to stay narrow. Condition 2 ensures us that the beam propagates over a sufficiently large distance and remains intense. Finally 3 ensures us that the field is not zero in its core. Then we define multiple filaments as a beam composed of a limited number of filaments.

Definition 2.3. We say that a solution is called K -multiple filament if it possesses K z_k -filaments (Fig. 5) of lengths $(L_k)_{k=1,\dots,K}$ and diameters $(\delta_k)_{k=1,\dots,K}$ propagating respectively in the directions $\mathbf{z}_1, \dots, \mathbf{z}_K$ in \mathbb{R}^3 if for all $k \in \{1, \dots, K\}$, each z_k -filament is a single filament of length L_k and diameter δ_k .

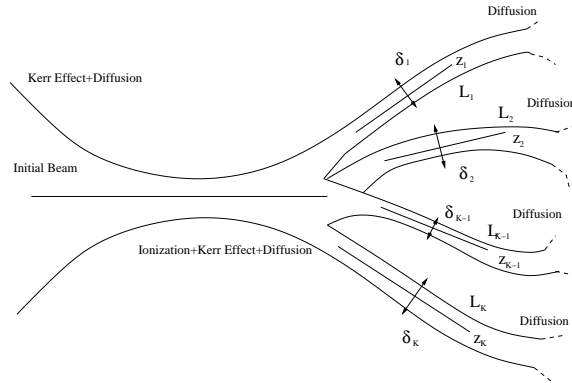


Figure 5: Evolution of multiple filament envelope.

Again, these general geometric definitions are supposed to describe several kinds of filament envelopes, usually observed experimentally and numerically, but is not exhaustive. See for instance [10, 12, 14]. Note that these structures are very complex and still not totally understood, which motivates this work. To our knowledge, there is no rigorous general proof of prediction of filamentation for the nonlinear wave or nonlinear Schrödinger equations, even if some incomplete arguments exist (see for instance [14] or [23]) or prediction on some very particular cases. However numerical observations exhibited solutions having a filament-like behavior.

Remark 2.4. From the nonlinear wave equation (2.18), we can derive a nonlinear Schrödinger equation using the slowly varying envelope approximation (SVEA) in the paraxial approximation. Suppose that \mathbf{E} can be written as

$$\mathcal{E}(\mathbf{r},t)\exp(i(k_z - \omega t))\mathbf{e}_y,$$

we obtain by slowly envelope approximation on the wave equation (see [23] for instance) and in the referential $z' = z, t' = t - z/c$ with $\mathbf{p} = (x, y, z')^T$

$$\partial_{z'}\mathcal{E}(\mathbf{p},t') - \frac{i}{2k_z}\Delta_{\perp}\mathcal{E}(\mathbf{p},t') = \frac{\delta n(|\mathcal{E}|^2, \rho)}{n_0}\mathcal{E}(\mathbf{p},t'). \tag{2.34}$$

The term δn is a nonlinear refraction index taking into account the Kerr and the plasma effects, and can be modeled using (2.19), (2.20) as ([10] or [22])

$$\frac{\delta n(|\mathcal{E}|^2, \rho)}{n_0}\mathcal{E} = -i\frac{k_0}{2n_0\rho_c}\rho\mathcal{E} + ik_0n_2|\mathcal{E}|^2\mathcal{E}, \tag{2.35a}$$

$$\partial_{t'}\rho = \sigma_K|\mathcal{E}|^{2K}\rho_{\text{atm}}, \tag{2.35b}$$

where $K = \langle U_i/\hbar\omega_0 + 1 \rangle$ (U_i ionization potential of the medium) is the number of photons involved in the multiphoton ionization, σ_K the coefficient of the multiphoton ionization rate, ρ_{atm} the neutral atom density (see [10]). Note that without plasma term,

the existence of solutions in H^1 is a particular case of [24]. For \mathcal{E}_0 in H^1 a solution in $\mathcal{C}(z_0, z_f; H^1)$ exists for z_f infinite or z_f finite such that the L^2 norm of \mathcal{E} tends to infinity when z tends to z_f .

The evolution process of filamentation is roughly the following for NLSs. The Kerr effect modeled by $ik_0 n_2 |\mathcal{E}|^2 \mathcal{E}$ has a self-focusing effect (it amplifies the focusing of a Gaussian beam), so that $|\mathcal{E}|$ increases and the gas is partially ionized so that free electron density ρ increases. When ρ increases the defocusing effect due to $-i(k_0/2n_0\rho_c)\rho\mathcal{E}$ makes $|\mathcal{E}|$ decrease. Over long distances filaments may be created (if an equilibrium is reached). In a more formal way the process can be described as follows. We first take an initial data defined by $\rho(\cdot, 0) = 0$ (when initially the gas is not ionized) and the initial electric field envelope, is the following Gaussian beam (details can for instance be found in [25])

$$\mathcal{E}_0(\mathbf{r}_\perp, t', z'=0) = \sqrt{I_0} \exp\left(-\frac{\|\mathbf{r}_\perp\|^2}{w_0^2} - i\frac{k_0\|\mathbf{r}_\perp\|^2}{2f}\right) \exp\left(-\frac{t'^2}{t_p^2}\right), \quad (2.36)$$

where f is the curvature radius, w_0 is the beam waist, t_p the pulse duration, and $\rho(\mathbf{r}_\perp, t', z'=0) = 0$. Starting from

$$\partial_{z'} \mathcal{E} = \frac{i}{2k_z} \Delta_\perp \mathcal{E} + ik_0 n_2 |\mathcal{E}|^2 \mathcal{E} - \frac{ik_0}{2n_0 \rho_c} \rho \mathcal{E}, \quad (2.37)$$

we multiply this equation by $\bar{\mathcal{E}}$, integrate by parts in $d\mathbf{r}_\perp = (x, y)^T$, leading to

$$\begin{aligned} & \partial_{z'} \int d\mathbf{r}_\perp |\mathcal{E}|^2 + 2i \int d\mathbf{r}_\perp \text{Im}(\bar{\mathcal{E}} \partial_{z'} \mathcal{E}) \\ &= -\frac{i}{k} \int d\mathbf{r}_\perp |\nabla_\perp \mathcal{E}|^2 + 2ik_0 n_2 \int d\mathbf{r}_\perp |\mathcal{E}|^4 - \frac{ik_0}{n_0 \rho_c} \int d\mathbf{r}_\perp \rho |\mathcal{E}|^2. \end{aligned}$$

We now denote by

$$\|\mathcal{E}\|_\perp^2 = \int d\mathbf{r}_\perp |\mathcal{E}|^2.$$

By taking the real and imaginary parts, we deduce that $\int d\mathbf{r}_\perp \bar{\mathcal{E}} \partial_{z'} \mathcal{E}$ is purely imaginary,

$$\partial_{z'} \|\mathcal{E}\|_\perp^2 = 0, \quad (2.38a)$$

$$\frac{1}{k} \|\nabla_\perp \mathcal{E}\|_\perp^2 - 2k_0 n_2 \|\mathcal{E}\|_\perp^4 + \frac{k_0}{n_0 \rho_c} \|\sqrt{\rho} \mathcal{E}\|_\perp^2 + 2 \int d\mathbf{r}_\perp \bar{\mathcal{E}} \partial_{z'} \mathcal{E} = 0, \quad (2.38b)$$

$$\partial_{t'} \rho = \sigma_K |\mathcal{E}|^{2K} \rho_{\text{atm}}, \quad (2.38c)$$

with

$$\partial_{t'} \rho = \sigma_K |\mathcal{E}|^{2K} \rho_{\text{atm}}.$$

We of course recognize the power conservation. We now apply a similar approach multiplying by $\partial_{z'}\bar{\mathcal{E}}$ integrating by parts and taking the real part. This leads this time to

$$\frac{1}{4k_z}\partial_{z'}\|\nabla_{\perp}\mathcal{E}\|_{\perp}^2 - \frac{k_0n_2}{4}\partial_{z'}\|\mathcal{E}\|_{\perp}^4 + \frac{k_0}{2}n_0\rho_c \int d\mathbf{r}_{\perp}\rho\partial_{z'}|\mathcal{E}|^2 = 0, \quad (2.39)$$

that we can rewrite

$$\partial_{z'}\|\nabla_{\perp}\mathcal{E}\|_{\perp}^2 - k_zk_0n_2\partial_{z'}\|\mathcal{E}\|_{\perp}^4 + \frac{2k_zk_0}{n_0\rho_c}\partial_{z'} \int d\mathbf{r}_{\perp}\rho|\mathcal{E}|^2 - \frac{2k_zk_0}{n_0\rho_c} \int d\mathbf{r}_{\perp}|\mathcal{E}|^2\partial_{z'}\rho = 0,$$

that is

$$\|\nabla_{\perp}\mathcal{E}\|_{\perp}^2 - k_zk_0n_2\|\mathcal{E}\|_{\perp}^4 + \frac{2k_zk_0}{n_0\rho_c}\|\sqrt{\rho}\mathcal{E}\|_{\perp}^2 - \frac{2k_zk_0}{n_0\rho_c} \int d\mathbf{r}|\mathcal{E}|^2\partial_{z'}\rho = \text{constant}.$$

For all \mathbf{r} and t these equalities are satisfied by the model ensuring an equilibrium between Kerr, diffusion and plasma effects. We note that $\|\nabla_{\perp}\mathcal{E}\|_{\perp}^2$ increases with $\|\mathcal{E}\|_{\perp}^4$ corresponding to a focusing when the laser intensity increases, and decreases because of the plasma term when the ionization increases.

Remark 2.5. Note that working in polar coordinates, Skarka et al. [26] have been able to identify filaments (more precisely OVS and LOVS that have been described in the introduction) writing $\mathcal{E}(x,y,z,t)$ in cylinder coordinates as $A(r)\exp(im\theta + i\beta z)$, so that

$$A''(r) + \frac{1}{r}A'(r) - \left(\frac{m^2}{r^2} + 2\beta k_z\right)A(r) = 2ik_zS_A.$$

The laser beam power is given by

$$\mathcal{P} = 2\pi \int A(r)^2 dr.$$

S_A can be naturally be expressed as a power sum of A . The solution is dependent of m that corresponds to the eigenmode.

More generally, many numerical simulations using model (2.34), (2.35) have exhibited filaments. See again [10] or [12] for a full bibliography on these simulations.

As proving analytically that the WASP or Maxwell-Schrödinger models can exhibit filament-like structure is very challenging (due to the complexity of the mathematical equations), we propose a numerical study of the model (Maxwell-Schrödinger) for the propagation of intense, short and high frequency Gaussian-like beam propagation in a gas.

3 Numerical simulations

We perform some numerical simulations of intense, ultrashort and high frequency electromagnetic fields propagating in a dense H_2^+ -gas. In the following simulations, we will work under the Born-Oppenheimer approximation. We then fix the internuclear distance that we will denote by R (that is $R' = R = \text{constant}$). The chosen incoming field is a Gaussian beam (3.1), that has the property to focus on a very short distance (focusing and defocusing). The interest of such a pulse is that it will allow us to compare efficiently the pulse thickness and intensity in gas and in vacuum. Moreover this is typically the kind of pulses that is experimentally used in laboratory. The equations that are solved are (2.4a), that is the global Maxwell-Schrödinger model, where the plasma equation is not included. As discussed above this model is still relevant when the pulse time duration is small enough (as plasma effects are included). Indeed molecule wavefunction is mainly not absorbed at the TDSE computational domain boundaries, so that "free electrons" (or electron far enough from the nuclei) are almost totally treated by the TDSEs. For longer pulses the plasma equation should be added and numerical simulations will be presented in a forthcoming paper. We suppose that 5 initial components are non-zero ($\mathbf{E}_0, \mathbf{B}_0$),

$$\left\{ \begin{array}{l} E_x = iE_0 \varepsilon^2 \frac{4Q^2 xy}{w_0^2} \psi_0 e^{i(\omega t_0 - kz)}, \\ E_y = -iE_0 \psi_0 \left(1 - 2Q \varepsilon^2 \left(i + \frac{2Qy^2}{w_0^2} \right) \right) e^{i(\omega t_0 - kz)}, \\ E_z = iE_0 \left(\varepsilon \frac{2Qy}{w_0} \psi_0 - \frac{1}{k^2} \frac{\partial^2 \psi_0}{\partial z \partial y} \right) e^{i(\omega t_0 - kz)}, \\ B_x = iE_0 \left(\psi_0 - \frac{1}{k} \frac{\partial \psi_0}{\partial z} \right) e^{i(\omega t_0 - kz)}, \\ B_y = 0, \\ B_z = -iE_0 \varepsilon \frac{2Qx}{w_0} \psi_0 e^{i(\omega t_0 - kz)}, \end{array} \right. \quad (3.1)$$

where w_0 is the beam waist, and $z_R = kw_0^2/2$ the Rayleigh range. Moreover

$$\psi_0(r, z) = \frac{w_0}{w} \exp\left(-\frac{r^2}{w^2}\right) \exp\left(i\left(\phi_R - \frac{r^2 z}{w^2 z_R}\right)\right), \quad w = w_0 \sqrt{1 + z/z_R},$$

$$Q = \frac{1}{z/z_R + i}, \quad \phi_R = \tan^{-1}\left(\frac{z}{z_R}\right), \quad \varepsilon = \frac{1}{kw_0}.$$

More precisely our initial data is the real part of \mathbf{E}_0 and \mathbf{B}_0 defined above. We will see in the following simulations, that as expected the focus is obtained on very short distances: $z_R \leq 5 \mu m$ (in fact, even with $E_x = E_z = B_z = 0$ at $t = t_0 = 0$). The other physical data are as follows:

- the laser pulse possesses 5–6 cycles;
- the propagation length in the gas is $\sim 10 \mu m$;

- the total length of the domain in z is $\sim 25\mu\text{m}$;
- the transverse window size is $\sim 10\mu\text{m} \times 10\mu\text{m}$.

The numerical approach is the one presented in [2], where the gas domain is divided in small cells of gas denoted by Δv (corresponding the Ω_i 's of Section 2) and in which we solve 1 TDSE, representing the $\mathcal{N}\text{vol}(\Delta v)$ molecules of the cell. In practice, 3d Maxwell's equations are solved in parallel with $\sim 140,000$ 1d TDSEs, see Fig. 6 and [27]. Solving 1d TDSEs do not allow us to capture all the laser-molecule interactions but allows us to consider "large" gas domains. The orientation of the molecule has been chosen in order to produce the highest harmonics and nonlinearities (see [28]). We can justify this uniform orientation by the common process in experimental physics, consisting of using a pumping laser pulse that polarizes all the molecules in the same direction before the interaction with the probe-pulse. However, random orientation x, y, z , can easily be implemented within the numerical code. More complex interactions would necessitate the use of 2d or 3d Schrödinger equations (also simple to implement, but then would lead to a much higher computational time).

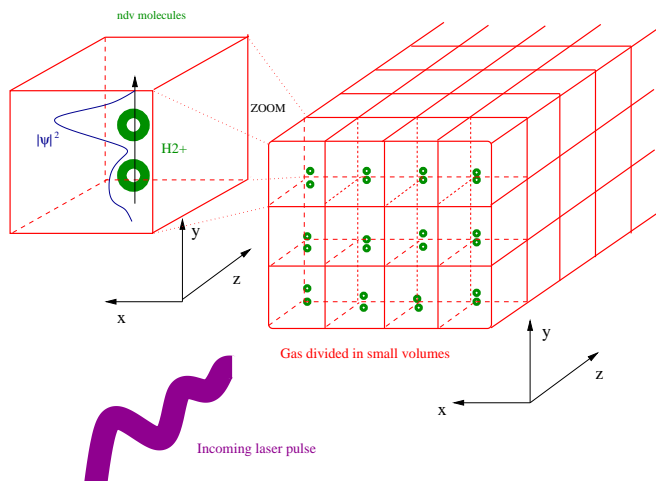


Figure 6: Computational geometry.

We represent at different times $(t_k)_k$, the transverse cut of the pulse at $(z_k)_k$ such that $|E_y(0,0,z,t_k)|$ is maximal at z_k on (Oz) . In other words,

- at t_k fixed, and we denote

$$|E_y|_\infty = \max_z |E_y(0,0,z,t_k)|$$

the maximal value on the (Oz) axis, reached at z_k ;

- we represent $E_y(x,0,z_k,t_k)/|E_y|_\infty$ to have normalized graphs, in order to compare with the propagation in vacuum.

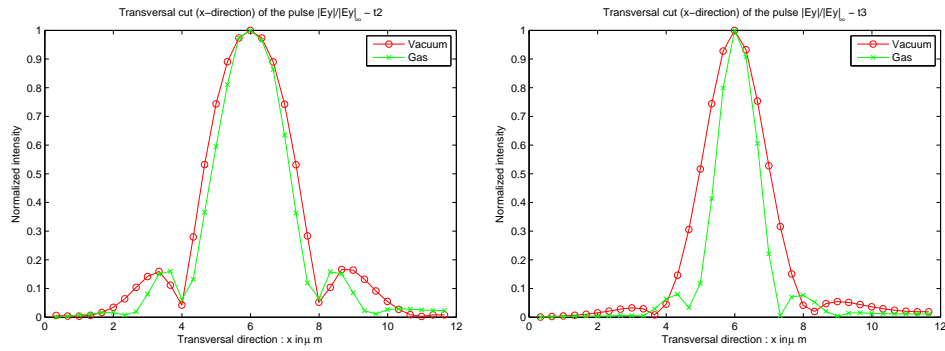


Figure 7: Pulse thickness during propagation $3.2\mu\text{m}$, $1\mu\text{m}$ before the waist, and $I_{\text{max}} \sim 6 \times 10^{14} \text{W}\cdot\text{cm}^{-2}$.

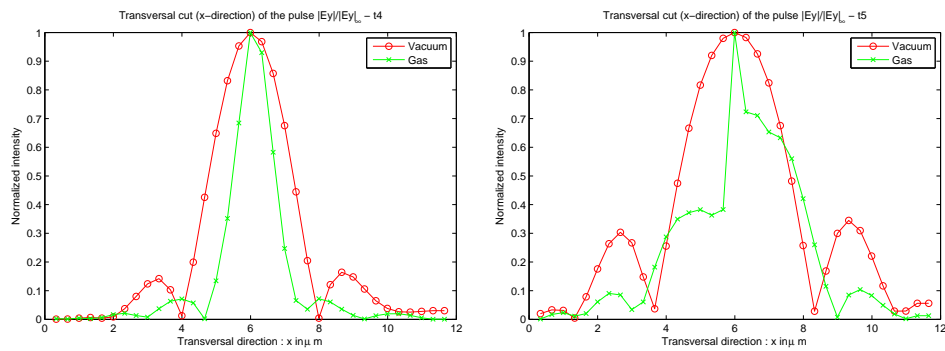


Figure 8: Pulse thickness during propagation $1.5\mu\text{m}$, $4\mu\text{m}$ after the waist, and $I_{\text{max}} \sim 6 \times 10^{14} \text{W}\cdot\text{cm}^{-2}$.

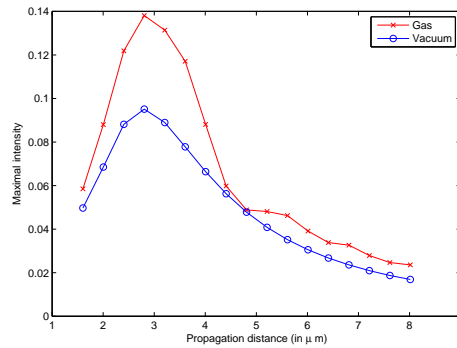


Figure 9: Comparison of maximal intensity for $I_{\text{max}} = 6 \times 10^{14} \text{W}\cdot\text{cm}^{-2}$, $\mathcal{N} = 3 \times 10^{20} \text{mol}\cdot\text{cm}^{-3}$ as a function of propagation length.

With the following data: $I_{\text{max}} \sim 6 \times 10^{14} \text{W}\cdot\text{cm}^{-2}$, $\mathcal{N} \sim 3 \times 10^{20} \text{mol}\cdot\text{cm}^{-3}$ and with $w_0 \sim 1.5\lambda_0$ (where λ_0 is the incoming pulse wavelength), we obtain the following transverse cuts on Figs. 7-9 that clearly make appear an amplification of the laser pulse focusing compared to vacuum and an increasing of the intensity, which corresponds exactly to the Kerr effect (self-focusing).

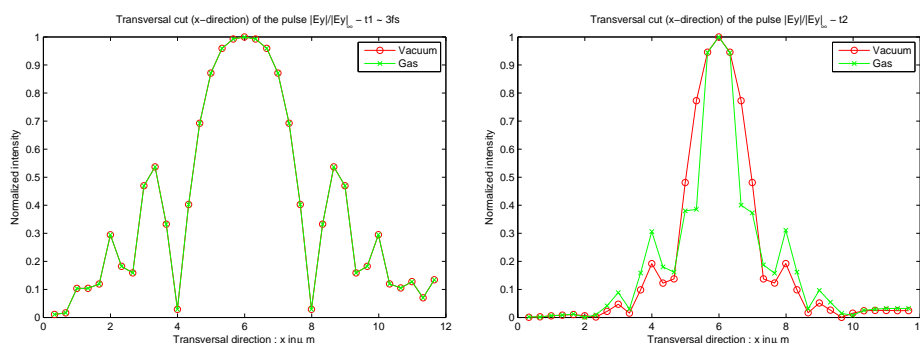


Figure 10: Pulse thickness during propagation $6\mu\text{m}$, $2.8\mu\text{m}$ before the waist, and $I_{\text{max}} \sim 2 \times 10^{16} \text{W}\cdot\text{cm}^{-2}$.

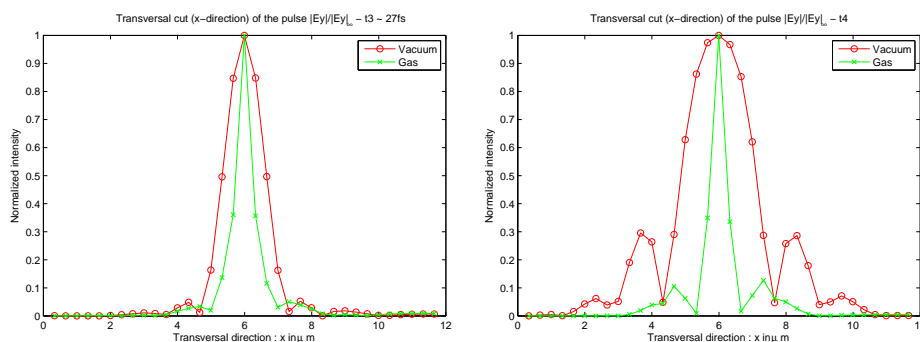


Figure 11: Pulse thickness during propagation $0.5\mu\text{m}$, $4.5\mu\text{m}$ after the waist, and $I_{\text{max}} \sim 2 \times 10^{16} \text{W}\cdot\text{cm}^{-2}$.

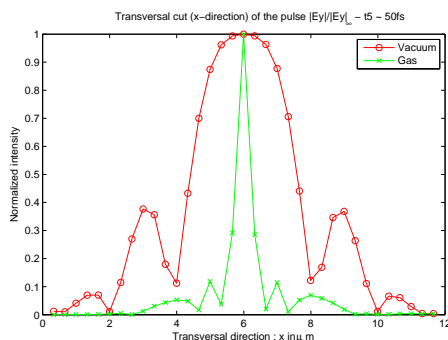
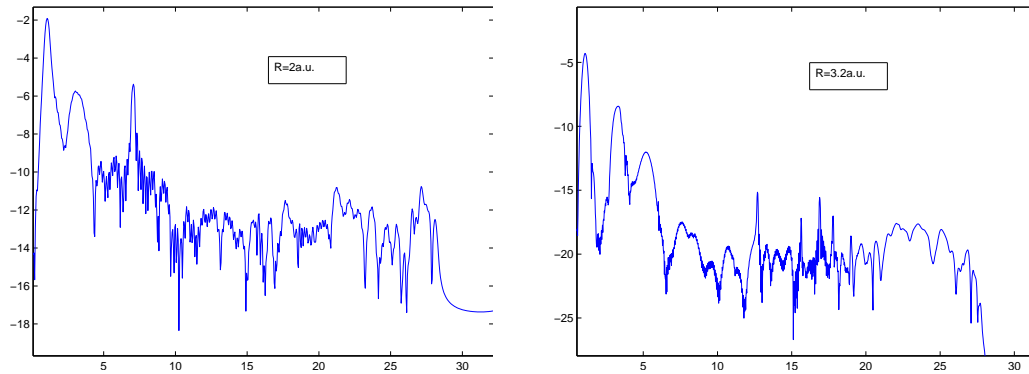
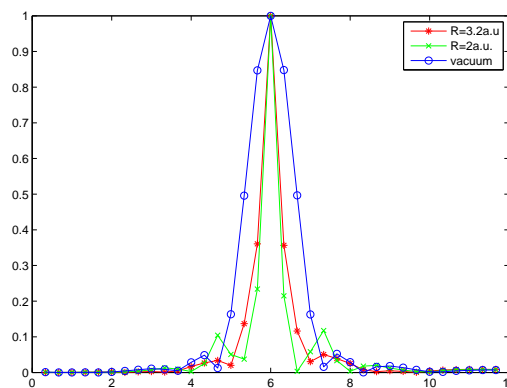


Figure 12: Pulse thickness during propagation $7\mu\text{m}$ after the waist, and $I_{\text{max}} \sim 2 \times 10^{16} \text{W}\cdot\text{cm}^{-2}$.

As expected, if we increase the intensity ($I_{\text{max}} \sim 2 \times 10^{16} \text{W}\cdot\text{cm}^{-2}$) of the pulse, the focusing is also amplified in the medium ($\mathcal{N} \sim 3 \times 10^{20} \text{mol}\cdot\text{cm}^{-3}$), see Figs. 10-12. We note in particular, that after the waist the pulse remains narrow, which is a feature of filaments.

The maximal intensity is ~ 2.5 times greater than in vacuum for the same propagation length and note that the ratio increases with the molecular density. We however suspect this ratio to be under-estimated by the model.

Figure 13: Electric field harmonics as a function of ω/ω_0 for $R=2.a.u.$, $R=3.2a.u.$.Figure 14: Electric field transverse cut in the waist for $R=2.a.u.$, $R=3.2a.u.$, for $I_{\max}=6 \times 10^{14} \text{W} \cdot \text{cm}^{-2}$.

Remark 3.1. In Fig. 14, we compare the electric field harmonics in the waist region for $I_{\max}=6 \times 10^{14} \text{W} \cdot \text{cm}^{-2}$, and the 5-cycle pulse, for two different internuclear distances $R=2.a.u.$ and $R=3.2a.u.$. As expected, the third harmonic ($\chi^{(3)}$) is more intense than the seventh one ($\chi^{(7)}$) for $R=3.2a.u.$ (due to 3-photon resonance, [28] for instance), Fig. 13. However and as observed in Fig. 14, the pulse width seems to be weakly dependent on R (for the chosen set of physical data).

These numerical results make appear structures that could be identified as filaments as the pulse thickness keeps a narrowness after the waist. Note again that due to the fact that the considered pulses are very short it was not necessary to include the plasma equation in the simulations (free electrons are mainly included in the TDSEs). Moreover it was confirmed numerically that the transmitted electric field possesses high order harmonics (Fig. 13) and nonlinearities, in particular the third order one (Kerr effect). A study of high harmonic effects is in progress as well as more complete tests. Numerical simulations with inclusion of the plasma equation in the model have been performed and show clearly filament-like behaviors, in particular the defocusing effect of the plasma of free electrons. These results will be presented in a forthcoming paper.

4 Conclusions

In this paper, we have first proven the existence and uniqueness of weak solutions for the Maxwell-Schrödinger model presented in [2] and describing intense and short laser-gas interaction and propagation. Using classical functional analysis tools, we have in particular proven the conservation in time of the initial data regularity. It was remarked in this paper, that the Maxwell-Schrödinger model is no more appropriate for long ($\geq 20fs$) and intense pulses, as free electron effects are then badly described. We then have added to the model a plasma equation based on the density of free electrons absorbed at the boundary of the TDSE computational domains. Such an equation allows in particular to precisely (as it is an *ab initio* free electron description) include plasma defocusing effects, experimentally observed. Some elements for deriving a nonlinear wave equation from the WASP model has also been discussed allowing a purely macroscopic (then much less computational costly) description of the gas response. Finally some high performance computations have been performed in order to validate the model. In particular the performed simulations have brought to light the first observation (to our knowledge) of a self-focusing effect (due to the 3rd nonlinearity at least, Kerr), with an *ab initio* gas description. Moreover it has been observed that during the propagation, the pulse thickness remains relatively narrow compared to vacuum as expected for filamentation. A complete comparison of the pulse thickness depending of the internuclear distance is still to be performed even if some preliminary observations have been provided in this paper. Additional tests are currently performed to confirm these effects on longer pulses where much denser plasmas of free electrons will be considered. These results will be presented in a forthcoming paper. In order to link our study to existing works on filamentation, a scale transformation ($x^* = Lx, t^* = Tt, \dots$) has to be performed (work in progress) to consider large domains (more than 1 meter). Several interesting questions regarding the WASP model are still open such as, in particular, a rigorous proof that it can analytically predict filament-like structures.

Acknowledgments

We thank Compute Canada for access to multiprocessor supercomputers for the simulations reported here.

References

- [1] E. Lorin, S. Chelkowski and A. Bandrauk, A Maxwell-Schrödinger model for non-perturbative laser-molecule interaction and some methods of numerical computation, In High-Dimensional Partial Differential Equations in Science and Engineering, Volume 41 of CRM Proc. Lect. Notes., pages 161–182, Amer. Math. Soc., Providence, RI, 2007.
- [2] E. Lorin, S. Chelkowski and A. Bandrauk, A numerical Maxwell-Schrödinger model for laser-matter interaction and propagation, Comput. Phys. Comm., 177(12) (2007), 908–932.

- [3] E. Lorin, S. Chelkowski and A. Bandrauk, Mathematical modeling of boundary conditions for laser-molecule time dependent Schrödinger equations and some aspects of their numerical computation, one-dimensional case, *Num. Methods. Partial. Differ. Equations*, 25(1) (2009), 110–136.
- [4] E. Lorin, S. Chelkowski and A. Bandrauk, Propagation effects on attosecond pulse generation, Number art. No. 67332V in *Proceedings of SPIE–The International Society for Optical Engineering*, 2007.
- [5] E. Lorin, S. Chelkowski and A. Bandrauk, Attosecond pulse generation from aligned molecules-dynamics and propagation in H_2^+ , *New. J. Phys.*, 10 (2008), 025033.
- [6] M. Lewenstein, Ph. Balcou, M. Y. Ivanov, A. Huillier and P. B. Corkum, Theory of high-harmonic generation by low frequency laser fields, *Phys. Rev. A.*, 49(3) (1994), 2117–2132.
- [7] P.-B. Corkum, Plasma perspective on strong-field multiphoton ionization, *Phys. Rev. Lett.*, 71 (1993), 1994–1997.
- [8] E. Dumas, Global existence for Maxwell-Bloch systems, *J. Differ. Equations.*, 219(2) (2005), 484–509.
- [9] J. L. Joly, G. Métivier and J. Rauch, Global solutions to Maxwell equations in a ferromagnetic medium, *Ann. Henri Poincaré.*, 1(2) (2010), 307–340.
- [10] A. Couairon and A. Mysyrowicz, Organizing multiple femtosecond filaments in air, *Phys. Rep.*, 41(3) (2007), 47–189.
- [11] L. Baudouin, O. Kavian and J.-P. Puel, Regularity for a Schrödinger equation with singular potentials and application to bilinear optimal control, *J. Differ. Equations.*, 216(1) (2005), 188–222.
- [12] L. Bergé, S. Skupin, R. Nuter, J. Kasparian and J.-P. Wolf, Ultrashort filaments of light in weakly ionized, optically transparent media, *Rep. Pro. Phys.*, 70(10) (2007), 1633–1713.
- [13] L. Bergé, C. Gouédard, J. Schjodt-Eriksen and H. Ward, Filamentation patterns in kerr media vs. beam shape robustness, nonlinear saturation and polarization states, *Phys. D.*, 176 (2003), 181–211.
- [14] G. Fibich and B. Ilan, Vectorial and random effects in self-focusing and in multiple filamentation, *Phys. D.*, 157(1-2) (2001), 112–146.
- [15] T. Brabec and F. Krausz, Intense few-cycle laser fields: frontier of nonlinear optics, *Rev. Mod. Phys.*, 72 (2000), 545–591.
- [16] H.-M. Yin, Existence and regularity of a weak solution to Maxwell's equations with a thermal effect, *Math. Methods. Appl. Sci.*, 29(10) (2006), 1199–1213.
- [17] R. W. Boyd, *Nonlinear Optics*, Academic Press, 2nd edition, 2003.
- [18] S. Skupin and L. Bergé, Self-guiding of femtosecond light pulses in condensed media: Plasma generation versus chromatic dispersion, *Phys. D.*, 220 (2006), 14–30.
- [19] A. Bandrauk and S. Chelkowski, Dynamic imaging of nuclear wavefunctions with ultrashort UV laser pulses, *Phys. Rev. Lett.*, 87(27) (2001), 113–120.
- [20] S. Chelkowski, A. Bandrauk and P.-B. Corkum, Femtosecond coulomb explosion imaging of vibrational wave functions, *Phys. Rev. Lett.*, 82(17) (1999), 3416–3419.
- [21] A. D. Bandrauk, S. Chelkowski and H. S. Nguyen, Attosecond localization of electrons in molecules, *Int. J. Quant. Chem.*, 100(6) (2004), 834–844.
- [22] V. Skarka, N. B. Aleksić and V. I. Berezhiani, Evolution of singular optical pulses towards vortex solitons and filamentation in air, *Phys. Lett. A.*, 319(3-4) (2003), 317–324.
- [23] B. Bidégaray-Fesquet, *Hiérarchie de modèles en optique Quantique, De Maxwell-Bloch Schrödinger Non-linéaire*, Springer-Verlag, Berlin, *Mathématiques et Applications*, Vol. 49, edition, 2006.

- [24] R. T. Glassey, On the blowing up of solutions to the Cauchy problem for nonlinear Schrödinger equations, *J. Math. Phys.*, 18(9) (1977), 1794–1797.
- [25] J. C. Diels and W. Rudolph, *Ultrashort Laser Pulse Phenomena*, Academic Press, 2nd edition (Optics and Photonics Series) edition, 2006.
- [26] N. B., V. I. Berezhiani, V. Skarka and Aleksić, Dynamics of localized and nonlocalized optical vortex solitons in cubic-quintic nonlinear media, *Phys. Lett. E.*, 64 (2001), 057601.
- [27] E. Lorin and A. Bandrauk, Efficient parallel computing for laser-gas quantum interaction and propagation, 22th High Performance Computing Symposium, IEEE, pages 4–8, 2008.
- [28] G. Lagmago Kamta and A. Bandrauk, Three-dimensional time-profile analysis of high-order harmonic generation in molecules: Nuclear interferences in H_2^+ , *Phys. Rev. A.*, 71 (2005), 053407.